JOURNAL OF AGRICULTURAL AND FOOD CHEMISTRY

Agricultural and Environmental Chemistry

Rational Optimization and Action Mechanism of Novel Imidazole (or Imidazolium)-Labeled 1,3,4-Oxadiazole Thioethers as Promising Antibacterial Agents Against Plant Bacterial Diseases

Peiyi Wang, Ming-Wei Wang, Dan Zeng, Meng Xiang, Jia-Rui Rao, Qing-Qing Liu, Li-Wei Liu, Zhi-Bing Wu, Zhong Li, Baoan Song, and Song Yang

J. Agric. Food Chem., **Just Accepted Manuscript** • Publication Date (Web): 05 Mar 2019

ACS Publications

is published by the American Chemical Society. 1155 Sixteenth Street N.W., Washington, DC 20036

Rational Optimization and Action Mechanism of Novel Imidazole (or Imidazolium)-Labeled 1,3,4-Oxadiazole Thioethers as Promising Antibacterial Agents Against Plant Bacterial Diseases

Pei-Yi Wang [†] [a], Ming-Wei Wang [†] [a], Dan Zeng [a], Meng Xiang [a], Jia-Rui Rao [a], Qing-Qing Liu [a], Li-Wei Liu [a], Zhi-Bing Wu [a], Zhong Li [b], Bao-An Song* [a], Song Yang* [a,b]

[a] State Key Laboratory Breeding Base of Green Pesticide and Agricultural Bioengineering, Key Laboratory of Green Pesticide and Agricultural Bioengineering, Ministry of Education, Center for R&D of Fine Chemicals of Guizhou University, Guiyang, 550025, China.

[b] College of Pharmacy, East China University of Science & Technology, Shanghai, China 200237.

[†] The two authors contribute equally to this work.

* Corresponding author.

E-mail: jhzx.msm@gmail.com (S. Yang), songbaoan22@yahoo.com (B.-A Song).

Abstract

The emergence and wide spread of plant bacterial diseases that cause global production constraints have become major challenges to agriculture worldwide. To promote the discovery and development of new bactericides, imidazole-labeled 1,3,4-oxadiazole thioethers were first fabricated by integrating the crucially bioactive scaffolds of imidazole motif and 1,3,4-oxadiazole skeleton in a single molecular architecture. Subsequently, a superior antibacterial compound **A_6** was gradually discovered parading an excellent competence against plant pathogens *Xanthomonas oryzae* pv. *oryzae* and *Xanthomonas axonopodis* pv. *citri* with EC_{50} values of 0.734 and 1.79 μg/mL, respectively. These values were better than those of commercial agents bismerthiazol (92.6 μg/mL) and thiodiazole copper (77.0 μg/mL). Further modifying the imidazole moiety into imidazolium scaffold led to the discovery of an array of potent antibacterial compounds providing the corresponding minimum EC_{50} values of 0.295 and 0.607 μg/mL against the two strains. Moreover, a plausible action mechanism for attacking pathogens was proposed based on the concentration dependence of SEM, TEM, and fluorescence microscopy images. Given the simple molecular structures, easy synthetic procedure, and highly efficient bioactivity, imidazole (or imidazolium)-labeled 1,3,4-oxadiazole thioethers can be further explored and developed as promising indicators for the development of commercial drugs.

Keywords

1,3,4-oxadiazole, imidazole or imidazolium, antibacterial, action mechanism

41 **1. Introduction**

42 Plant diseases caused by invasive phytopathogenic bacteria are widespread and
43 virulent, and seriously threaten the output and quality of agricultural production
44 worldwide; moreover, they have become one of the overriding and urgent issues to be
45 addressed in agricultural production.[1-4] For example, bacterial leaf blight (BLB),
46 which is caused by the gram-negative pathogen *Xanthomonas oryzae* pv. *oryzae*
47 (*Xoo*), is an overwhelming disease occurring at any one of rice growth periods; it can
48 result in substantial production decrease of up to 80% under conditions favorable to
49 disease occurrence and spread.[5-10] Citrus bacterial canker, which is caused by a severe
50 and widespread gram-negative pathogen *Xanthomonas axonopodis pv. citri* (*Xac*), is
51 an rebellious disease that causes necrotic canker lesions in the fruit, stems, and leaves,
52 and can significantly decrease the fruit quality and yield.[11,12] Furthermore, climate
53 changes, such as rainfall and wind throughout the growth period aggravate the
54 infection and distribution of plant diseases, seriously promoting potential risks
55 associated with human health.[13,14] In view of the existing prevention and treatment
56 programs toward plant diseases, chemical control approaches employing bactericides
57 have become one of the most effective management strategies and have been
58 extensively developed due to the fast-acting property toward adversaries, low
59 investment from farmers, and easy operations on the crops.[2,15,16] However, the
60 long-term usage and abuse of existing traditional bactericides, such as streptomycin,
61 triazoles, bismerthiazol (**BT**), and thiodiazole copper (**TC**), have resulted in depressed
62 defenses against pathogens and the emergence of resistant pathogenic races.[3,5,10,16,17]

63 Moreover, investigation results have demonstrated that the explosion of resistance
64 will be extremely accelerated in just a few short years once the resistant pathogenic
65 race appears, assigning great challenges for us to manage this new circumstance.[18-20]
66 Thus, exploring and developing novel, simple structures possessing highly efficient
67 bioactivity and unique modes of action as alternative bactericides are needed.

68 Numerous studies have been extensively performed for searching highly efficient
69 molecular structures as antibacterial candidates, in which the biological effects of
70 various key skeletons have been carefully explored and highlighted.[7,21-24] Particularly
71 worth mentioning is 1,3,4-oxadiazole skeleton, which was promoted from the ring
72 closure of bisamides and can serve as surrogates for carboxylic acids, esters, and
73 amides due to its diverse competence to parade an array of biological activities
74 including antiviral, analgesic, antipsychotic, anti-allergic, antitumor, and
75 anti-inflammatory.[25-30] Especially, the antibacterial effects of
76 1,3,4-oxadiazole-tailored molecules were closely investigated on account of this
77 privileged structural motif, consequently opening a new avenue on the discovery of
78 novel, highly efficient bioactive substrates bearing 1,3,4-oxadiazole scaffolds in
79 antimicrobial chemotherapy.[7,16-18,31-33]

80 As another stimulating and capable key fragment in the exploration of novel
81 antimicrobial substances, the imidazole scaffold has been elaborately investigated for
82 its dramatic role in refurbishing the bioactivity of final target compounds.[34-37] For
83 example, Wang and co-workers reported and evaluated the antibacterial activity of a
84 series of imidazole-functionalized coumarin derivatives, and found that this designed

85 molecules exert good broad-spectrum antimicrobial abilities toward *Escherichia coli*,
86 *Staphylococcus aureus*, *Streptococcus agalactiae*, and *Flavobacterium cloumnare*.[38]
87 Meanwhile, imidazolium motif owning a cationic nitrogen atom derived from the
88 imidazole group has demonstrated a huge potential for improving drug development,
89 delivery, and efficacy due to its high affinity and feasible interactions toward
90 biological anionic components.[39-43] Simultaneously, Shamshina and colleagues
91 suggested that pharmaceutical industry should provide considerable attention to
92 explore and develop ionic liquid drugs in the future considering their superiorly
93 privileged performances serving as ideal and capable drugs against diseases.[44]
94 Inspired by the abovementioned studies, integrating the crucially bioactive scaffolds
95 of imidazole (or imidazolium) motif and 1,3,4-oxadiazole skeleton in a single
96 molecular architecture may motivate and promote the discovery and development of
97 new bactericides. To our knowledge, studies describing the general antibacterial
98 capability of imidazole (or imidazolium)-tagged 1,3,4-oxadiazole thioethers toward
99 plant pathogens are lacking. As a part of our ongoing program for exploring potent
100 alternative candidates, herein, a type of 1,3,4-oxadiazole thioethers owning imidazole
101 (or imidazolium) motifs with different alkyl lengths of chemical bridges was
102 constructed (Figure 1). The antibacterial activity toward devastating phytopathogens
103 *Xoo* and *Xac* was also evaluated. Furthermore, a plausible action mechanism for the
104 inhibitory activity of this kind of compounds would be proposed and investigated via
105 scanning electron microscopy (SEM), transmission electron microscopy (TEM), and
106 fluorescence microscopy (FM).

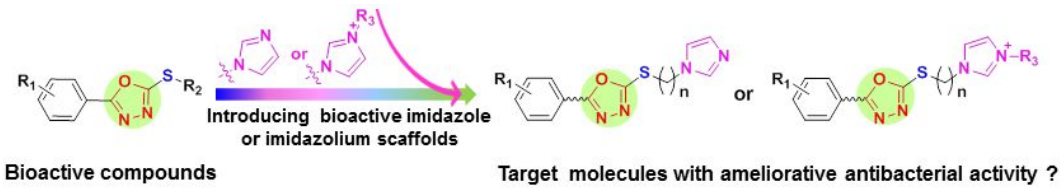

Figure 1. Design strategy for the target molecules.

2. Materials and methods

2.1 Instruments and chemicals

Nuclear magnetic resonance (NMR) spectra were obtained using a JEOL-ECX-500 apparatus. Chemical shifts were reported in parts per million (ppm) down field from TMS with the solvent resonance as the internal standard. Coupling constants (*J*) were reported in Hz and referred to apparent peak multiplications. SEM images were visualized and obtained using Nova Nano SEM 450. TEM measurements were carried out on a FEI Talos F200C electron microscope operating at an acceleration voltage of 120 kV. FM images were obtained using EVOS™ FL Auto Imaging System AMAFD1000.

2.2 *In vitro* antibacterial bioassay (turbidimeter test)

In our study, all the synthesized target compounds were evaluated for their antibacterial activities against *Xoo* and *Xac* by the turbidimeter test *in vitro*. Dimethylsulfoxide (DMSO) in sterile distilled water served as a blank control, whereas Bismerthiazol and Thiodiazole Copper served as positive controls.[7,17] Approximately 40 μL of solvent NB (1.5 g beef extract, 2.5 g peptone, 0.5 g yeast powder, 5.0 g glucose, and 500 mL distilled water; pH = 7.0–7.2) containing *Xoo* (or *Xac*), incubated on the phase of logarithmic growth, was added to 5 mL of solvent NB containing test compounds and positive control at different concentrations, such as

128 100 and 50 μg/mL (for preliminary bioassays), 20, 10, 5, 2.5, and 1.25 μg/mL or 10,
129 5, 2.5, 1.25, and 0.625 μg/mL (depending on the bioactivity of different compounds,
130 the concentrations were chosen in two times declining trend to make sure that the
131 EC_{50} values are inside the concentration ranges tested). The inoculated test tubes were
132 incubated at 28 ± 1 °C and continuously shaken at 180 rpm for 24-48 h until the
133 bacteria were incubated on the logarithmic growth phase. The growth of the cultures
134 was monitored on a microplate reader by measuring the optical density at 595 nm
135 (OD_{595}) given by turbidity-corrected values = $OD_{\text{bacterial wilt}} - OD_{\text{no bacterial wilt}}$, and the
136 inhibition rate I was calculated by $I = (C - T)/C \times 100\%$. C is the corrected turbidity
137 values of bacterial growth on untreated NB (blank control), and T is the corrected
138 turbidity values of bacterial growth on treated NB. By using the SPSS 17.0 software
139 and the obtained inhibition rates at different concentrations, a regression equation was
140 provided. The results of antibacterial activities (expressed by EC_{50}) against *Xoo* and
141 *Xac* were calculated from the equation and the value was within the concentration
142 ranges. The experiment was repeated thrice.

143 **2.3 Scanning electron microscopy (SEM)**

144 In this assay, 1.5 mL *Xoo* (or *Xac*) cells incubated at the logarithmic phase were
145 centrifuged and washed with phosphate-buffered saline (PBS, pH = 7.0) and
146 re-suspended in 1.5 mL of PBS buffer (pH = 7.0). Then, bacteria *Xoo* (or *Xac*) were
147 incubated with compounds $\mathbf{A_6}$ or $\mathbf{G_8}$ at different concentrations, and an equivalent
148 volume of DMSO (solvent control) for 4 h at room temperature. After incubation,
149 these samples were washed thrice with PBS (pH = 7.0). Subsequently, the bacterial

150 cells were fixed for 8 h at 4 °C with 2.5% glutaraldehyde, and then dehydrated with
151 graded ethanol series and pure tert-butanol (2 times with 10 min/time). Following
152 dehydration, samples were freez-dried, coated with gold, and visualized using Nova
153 Nano SEM 450.

154 **2.4 Synthesis for the intermediates and target compounds**

155 **2.4.1 General synthetic procedures for the target compounds A_n.**

156 **General synthetic procedures for the target compounds A_1.**

157 5-(2,4-dichlorophenyl)-1,3,4-oxadiazole-2-thiol **4** was prepared using our
158 previous approach.[20,27] 1-(Bromomethyl)-1*H*-imidazole (0.2 g, 1.21 mmol) was added
159 into a solution of 5 mL dimethyl formamide containing intermediate **4** (0.3 g, 1.21
160 mmol) and K_2CO_3 (0.18 g, 1.33 mmol) at room temperature for 2 h. After that, 50 mL
161 ethyl acetate was added into the mixture. The organic layer was washed by water,
162 saturated solution of ammonium chloride, dried with sodium sulfate, and followed by
163 the removal of the solvent under vacuum. The desired product $\mathbf{A_1}$ was purified by a
164 silica gel using CH_2Cl_2 and CH_3OH (40:1) as the eluent. A yellow solid, yield 76.9%,
165 m. p. 104.7-106.1 ℃; ^{1}H NMR (500 MHz, $CDCl_3$) δ 7.88–7.78 (m, 2H, Ar-6-H &
166 Imidazole-2-H), 7.53 (d, *J* = 2.1 Hz, 1H, Ar-3-H), 7.36 (dd, *J* = 8.5, 2.1 Hz, 1H,
167 Ar-5-H), 7.20 (s, 1H, Imidazole-5-H), 7.03 (d, *J* = 16.5 Hz, 1H, Imidazole-4-H), 5.80
168 (s, 2H, S-CH_2); ^{13}C NMR (126 MHz, $CDCl_3$) δ 164.3, 162.8, 138.5, 138.2, 133.9,
169 131.6, 131.3, 130.3, 127.8, 120.9, 119.5, 47.2; HRMS (ESI) $[M+H]^+$calcd for
170 $C_{12}H_8Cl_2N_4OS$: 326.9869, found: 326.9862.

171 **General synthetic procedures for the target compounds A_4.**

172 Intermediate **4** (0.3 g, 1.21 mmol) was added into a solution of 5 mL dimethyl
173 formamide containing K_2CO_3 (0.18 g, 1.33 mmol) and 1,4-dibromobutane (0.39 g,
174 1.82 mmol) at room temperature for 1 h. After that, 50 mL ethyl acetate was added

175 into the mixture. The organic layer was washed by water, saturated solution of
176 ammonium chloride, dried with sodium sulfate, and followed by the removal of the
177 solvent under vacuum. The crude residue was added into a solution containing
178 imidazole (1.12 mmol), NaH (1.54 mmol), and 5 mL dimethyl formamide. After
179 stirring the solution for 8 hours, 50 mL ethyl acetate was added. The organic layer
180 was washed by water, brine, dried with sodium sulfate, filtered, and followed by the
181 removal of the solvent under vacuum. Finally, the desired product was purified by a
182 silica gel using CH_2Cl_2 and CH_3OH (25:1) as the eluent. Title compound **A_4**, a light
183 yellow solid, m. p. 61.4-63.0 ℃, yield 71.7%; ^{1}H NMR (500 MHz, $CDCl_3$) δ 7.89 (d,
184 *J* = 8.5 Hz, 1H, Ar-6-H), 7.56-7.51 (m, 2H, Ar-3-H & Imidazole-2-H), 7.38 (dd, *J* =
185 8.5, 2.0 Hz, 1H, Ar-5-H), 7.07 (s, 1H, Imidazole-5-H), 6.94 (s, 1H, Imidazole-4-H),
186 4.01 (t, *J* = 6.9 Hz, 2H, N-CH_2), 3.30 (t, *J* = 7.1 Hz, 2H, S-CH_2), 2.08-1.93 (m, 2H,
187 N-CH_2<u>CH_2</u>), 1.88 (dt, *J* = 18.3, 7.8 Hz, 2H, S-CH_2<u>CH_2</u>); ^{13}C NMR (126 MHz,
188 $CDCl_3$) δ 165.1, 163.6, 138.3, 133.9, 131.7, 131.3, 127.8, 127.6, 121.5, 46.6, 31.9,
189 30.1, 26.6; HRMS (ESI) $[M+H]^+$calcd for $C_{15}H_{14}Cl_2N_4OS$: 369.0338, found:
190 369.0331.

191 The synthesis of compounds **A_5-A_8** were carried out as synthetic protocols of **A_4**.

192 **2.4.2 General synthetic procedures for the target compounds B_n.**

193 The synthesis of **B_4-B_6, B_8** were carried out as synthetic protocols of **A_4**, in which the
194 5-(2,4-dichlorophenyl)-1,3,4-oxadiazole-2-thiol was replaced by
195 5-(2,4-dichlorophenyl)-1,3,4-oxadiazol-2-ol.

196 **2-(4-(1*H*-imidazol-1-yl)butoxy)-5-(2,4-dichlorophenyl)-1,3,4-oxadiazole (B_4).**

197 A light yellow solid, yield 61.4% m. p. 53.8-55.0 ℃; ^{1}H NMR (500 MHz,
198 $CDCl_3$) δ 7.70 (d, *J* = 8.5 Hz, 1H, Ar-6-H), 7.51 (d, *J* = 2.0 Hz, 1H, Ar-3-H), 7.45 (s,
199 1H, Imidazole-2-H), 7.35 (dd, *J* = 8.5, 2.1 Hz, 1H, Ar-5-H), 7.03 (s, 1H,
200 Imidazole-5-H), 6.89 (t, *J* = 1.2 Hz, 1H, Imidazole-4-H), 3.99 (t, *J* = 6.8 Hz, 2H,

N-CH_2), 3.82 (t, J = 6.6 Hz, 2H, O-CH_2), 1.92-1.84 (m, 2H, N-$CH_2\underline{CH_2}$), 1.83-1.77 (m, 2H, O-$CH_2\underline{CH_2}$); ^{13}C NMR (126 MHz, $CDCl_3$) δ 153.0, 150.9, 138.0, 137.1, 133.4, 131.5, 130.6, 129. 8, 127.7, 121.1, 118.7, 46.3, 45.3, 28.0, 25.4; HRMS (ESI) $[M+H]^+$calcd for $C_{12}H_8Cl_2N_4O_2$: 353.0567, found: 353.0559.

2.4.3 General synthetic procedures for the target compounds C_n.

The synthesis of **C_5, C_6, C_8, C_{10}** were carried out as synthetic protocols of **A_4**, in which the 5-(2,4-dichlorophenyl)-1,3,4-oxadiazole-2-thiol was replaced by 5-(2,4-dichlorophenyl)-1,3,4-thiadiazole-2-thiol.

2-((5-(1*H*-imidazol-1-yl)pentyl)thio)-5-(2,4-dichlorophenyl)-1,3,4-thiadiazole (C_5). A light yellow solid, yield 88.9%, m. p. 99.0-100.9 ℃; ^{1}H NMR (500 MHz, $CDCl_3$) δ 8.23 (d, J = 8.6 Hz, 1H, Ar-6-H), 7.53 (d, J = 2.1 Hz, 1H, Ar-3-H), 7.46 (s, 1H, Imidazole-2-H), 7.38 (dd, J = 8.6, 2.1 Hz, 1H, Ar-5-H), 7.05 (s, 1H, Imidazole-5-H), 6.90 (s, 1H, Imidazole-4-H), 3.95 (t, J = 7.1 Hz, 2H, N-CH_2), 3.36 (t, J = 7.1 Hz, 2H, S-CH_2), 1.91-1.81 (m, 4H, N-$CH_2\underline{CH_2}$ & S-$CH_2\underline{CH_2}$), 1.56-1.41 (m, 2H, S-$(CH_2)_2\underline{CH_2}$); ^{13}C NMR (126 MHz, $CDCl_3$) δ 167.4, 162.7, 137.2, 133.0, 131.6, 130.4, 129.6, 128.0, 127.5, 118.8, 46.8, 33.6, 30.6, 28.8, 25.7; HRMS (ESI) $[M+H]^+$calcd for $C_{16}H_{16}Cl_2N_4S_2$: 399.0266, found: 399.0259.

2.4.4 General synthetic procedure for the intermediate 7.

5-(2,4-dichlorophenyl)-1,3,4-oxadiazole-2-thiol **4** (0.5 g, 2.02 mmol), and 80% $NH_2NH_2{\cdot}H_2O$ (0.25 g, 4.04 mmol) in 10 mL ethanol were stirred at 80 ℃ for 10 hours. After that, the solvent was removed under reduced pressure and followed by adding 5.0 mL water. The pH of the solution was adjusted into about 3 and resulted in a lot of precipitates which were filtered and dried to afford the intermediate **7**, a white solid, yield 91.3%, m. p. 179.6-181.1 ℃; ^{1}H NMR (500 MHz, DMSO-d_6) δ 14.02 (s,

225 1H, -SH), 7.86 (d, J = 2.0 Hz, 1H, Ar-3-H), 7.66 (d, J = 8.3 Hz, 1H, Ar-6-H), 7.62
226 (dd, J = 8.3, 2.0 Hz, 1H, Ar-5-H), 5.53 (s, 2H, $-NH_2$); ^{13}C NMR (126 MHz,
227 DMSO-d_6) δ 166.9, 148.0, 136.3, 134.5, 133.8, 129.3, 127.4, 124.2; MS (ESI): m/z =
228 260 [$M+H^+$].

229 **2.4.5 General synthetic procedures for the target compounds D_6.**

230 The synthesis of compound **D_6** were carried out as synthetic protocols of **A_4**. A
231 light yellow solid, yield 71.0%, m. p. 60.1-62.1 ℃; ^1H NMR (500 MHz, $CDCl_3$) δ
232 7.58 (d, J = 2.0 Hz, 1H, Ar-3-H), 7.48 (s, 1H, Imidazole-2-H), 7.06 (d, J = 3.5 Hz, 1H,
233 Ar-6-H), 7.01 (s, 1H, Imidazole-5-H), 6.87 (s, 1H, Imidazole-4-H), 6.54 (dd, 1H, J =
234 8.3, 2.0 Hz, 1H, Ar-5-H), 3.90 (t, J = 7.1 Hz, 2H, $N-CH_2$), 3.22 (t, J = 7.3 Hz, 2H,
235 $S-CH_2$), 1.81-1.72 (m, 4H, $N-CH_2\underline{CH_2}$ & $S-CH_2\underline{CH_2}$), 1.44 (dt, J = 15.2, 7.6 Hz, 2H,
236 $N-(CH_2)_2\underline{CH_2}$), 1.30 (dt, J = 15.1, 7.7 Hz, 2H, $S-(CH_2)_2\underline{CH_2}$); ^{13}C NMR (126 MHz,
237 $CDCl_3$) δ 163.9, 158.5, 145.7, 139.0, 137.1, 129.3, 118.8, 113.9, 112.2, 46.9, 32.4,
238 30.8, 29.0, 27.9, 25.9; HRMS (ESI) $[M+H]^+$calcd for $C_{17}H_{20}Cl_2N_6S$: 411.0920, found:
239 411.0926.

240 **2.4.6 General synthetic procedures for the target compounds E_n.**

241 The synthesis of **E_1-E_{14}** were carried out as synthetic protocols of **A_4**, in which the
242 5-(2,4-dichlorophenyl)-1,3,4-oxadiazole-2-thiol was replaced with various
243 5-substituted-1,3,4-oxadiazole-2-thiol.

244 **2-((6-(1*H*-imidazol-1-yl)hexyl)thio)-5-(3-nitrophenyl)-1,3,4-oxadiazole (E_1).**
245 A yellow liquid, yield 71.1%; ^1H NMR (500 MHz, $CDCl_3$) δ 8.82 (t, J = 1.8 Hz, 1H,
246 Ar-2-H), 8.52-8.28 (m, 2H, Ar-4,6-H), 7.72 (t, J = 8.0 Hz, 1H, Ar-5-H), 7.47 (s, 1H,
247 Imidazole-2-H), 7.05 (s, 1H, Imidazole-5-H), 6.91 (s, 1H, Imidazole-4-H), 3.94 (t, J =
248 7.1 Hz, 2H, $N-CH_2$), 3.31 (t, J = 7.1 Hz, 2H, $S-CH_2$), 1.89-1.78 (m, 4H, $N-CH_2\underline{CH_2}$ &
249 $S-CH_2\underline{CH_2}$), 1.60-1.45 (m, 2H, $N-(CH_2)_2\underline{CH_2}$), 1.42-1.31 (m, 2H, $S-(CH_2)_2\underline{CH_2}$); ^{13}C

250 NMR (126 MHz, $CDCl_3$) δ 165.9, 163.9, 148.8, 137.2, 132.3, 130.6, 129.6, 126.2,
251 125.4, 121.6, 118.9, 47.0, 32.5, 31.0, 29.1, 28.2, 26.1; HRMS (ESI) $[M+H]^+$calcd for
252 $C_{17}H_{19}N_5O_3S$: 374.1281, found: 374.1272.

253 **2.4.7 General synthetic procedures for the target compounds F_n.**

254 The synthesis of **F_1-F_6** were carried out as synthetic protocols of **A_4**, in which the
255 imidazole was replaced with diethylamine, pyrazole, morpholine, 1,2,4-triazole,
256 piperidine, and 4-hydroxypyridine, respectively.

257 **2-((6-(1*H*-pyrazol-1-yl)hexyl)thio)-5-(2,4-dichlorophenyl)-1,3,4-oxadiazole**
258 **(F_1).** A light yellow liquid, yield 48.0%; ^{1}H NMR (500 MHz, $CDCl_3$) δ 7.89 (d, *J* =
259 8.5 Hz, 1H, Ar-6-H), 7.55 (d, *J* = 2.0 Hz, 1H, Ar-3-H), 7.48 (d, *J* = 1.7 Hz, 1H,
260 Pyrazole-5-H), 7.38 (dd, *J* = 8.5, 2.0 Hz, 1H, Ar-5-H), 7.37 (d, *J* = 2.3 Hz, 1H,
261 Pyrazole-3-H), 6.22 (t, *J* = 2.0 Hz, 1H, Pyrazole-4-H), 4.12 (t, *J* = 7.1 Hz, 2H, N-CH_2),
262 3.27 (t, *J* = 7.3 Hz, 2H, S-CH_2), 1.92-1.80 (m, 4H, N-CH_2<u>CH_2</u> & S-CH_2<u>CH_2</u>), 1.49 (dt,
263 *J* = 15.0, 7.3 Hz, 2H, N-$(CH_2)_2$<u>CH_2</u>), 1.38-1.29 (m, 2H, S-$(CH_2)_2$<u>CH_2</u>); ^{13}C NMR (126
264 MHz, $CDCl_3$) δ 165.6, 163.4, 139.3, 138.1, 133.9, 131.7, 131.3, 129.0, 127.7, 121.6,
265 105.4, 52.0, 326, 30.4, 29.3, 28.2, 26.2; HRMS (ESI) $[M+H]^+$calcd for
266 $C_{17}H1_8Cl_2N_4OS$: 397.0651, found: 397.0644.

267 **2.4.8 General synthetic procedures for the target compounds G_n.**

268 2-((6-(1*H*-imidazol-1-yl)hexyl)thio)-5-(2,4-dichlorophenyl)-1,3,4-oxadiazole **A_6**
269 (0.17 g, 0.43 mmol) and methyl iodide (0.18 g, 1.29 mmol) were stirred in 4 mL
270 CH_3CN at 70 ℃ for 12 h. After that, the excess CH_3CN was removed under reduced
271 pressure. Finally, the desired product was purified by a silica gel using CH_2Cl_2 and
272 CH_3OH (25:1) as the eluent. Titile compound **G_1**, a yellow liquid, yield 83.7%; ^{1}H
273 NMR (500 MHz, $CDCl_3$) δ 9.88 (s, 1H, Imidazole-2-H), 7.85 (d, *J* = 8.5 Hz, 1H,
274 Ar-6-H), 7.59 (t, *J* = 1.8 Hz, 1H, Ar-3-H), 7.54 (t, *J* = 1.6 Hz, 1H, Imidazole-4-H),

275 7.50 (d, J = 2.0 Hz, 1H, Imidazole-5-H), 7.36 (dd, J = 8.5, 2.1 Hz, 1H, Ar-5-H), 4.34
276 (t, J = 7.4 Hz, 2H, N-CH_2), 4.07 (s, 3H, N^+-CH_3), 3.24 (t, J = 7.4 Hz, 2H, S-CH_2),
277 1.94 (dt, J = 15.1, 7.6 Hz, 2H, N-$CH_2\underline{CH_2}$), 1.86-1.77 (m, 2H, S-$CH_2\underline{CH_2}$), 1.53-1.47
278 (m, 2H, N-$(CH_2)_2\underline{CH_2}$), 1.43-1.37 (m, 2H, S-$(CH_2)_2\underline{CH_2}$); ^{13}C NMR (126 MHz,
279 $CDCl_3$) δ 165.5, 163.2, 138.0, 136.6, 133.6, 131.6, 131.2, 127.7, 123.7, 122.5, 121.2,
280 50.0, 37.1, 32.3, 29.9, 28.9, 27.6, 25.4; HRMS (ESI) $[M-I]^+$calcd for $C_{18}H_{21}Cl_2N_4OS$:
281 411.0808, found: 411.0797.

282 The synthesis of compounds **G_2-G_{18}** were carried out as synthetic protocols of **G_1**.

283 **3. Results and discussion**

284 To study the fusion of imidazole skeleton toward bioactivity, a type of
285 imidazole-tailored 5-(2,4-dichlorophenyl)-1,3,4-oxadiazole thioethers (**A_n**) bridging
286 by various alkyl chains was constructed. Briefly, the crucial intermediate **4** possessing
287 a 1,3,4-oxadiazole ring was prepared according to our previously described
288 approach[20,27] and was then reacted with 1-(bromomethyl)-1*H*-imidazole under the
289 alkaline condition to afford a title compound **A_1**. Meanwhile, the other compounds
290 (**A_n**, n = 4-8) were obtained by treating intermediates **4** with two-step consecutive
291 reactions with dibromo-substituted alkyls and imidazole. All the above-mentioned
292 compounds were characterized by ^{1}H NMR, ^{13}C NMR, and high-resolution mass
293 spectrometry (HRMS) (for detailed information, see Supplementary data). In this
294 study, turbidimeter test was performed to evaluate the antibacterial activities of **A_n**
295 against *Xoo* and *Xac* in *vitro*, and the commercial agricultural antibiotics **BT** and **TC**
296 were co-assayed as positive controls under the same condition.[7,20,27] As illustrated in
297 Table 1, appreciable antibacterial capability was observable and conferred after

integrating the imidazole motif into the target compounds compared with those of **BT** (92.6 μg/mL) and **TC** (121.8 and 77.0 μg/mL). This result suggested that imidazole scaffold can serve as an elaborate tailor to refurbish the bioactivity of final target compounds. A squint from the screening result revealed that antibacterial efficacy toward *Xoo* and *Xac* first increased and then decreased with manipulating the length of alkyl tailors and resulted in the minimal EC_{50} values of up to 0.734 and 1.79 μg/mL, respectively. This outcome indicated that even fine-tailoring the ratio of hydrophobicity/hydrophilicity patterns would affect their bioactivities. Based on the above result, the highly efficient antibacterial molecule $\mathbf{A_6}$ can be considered the secondary lead compound for searching even effectively high efficient antibacterial agents.

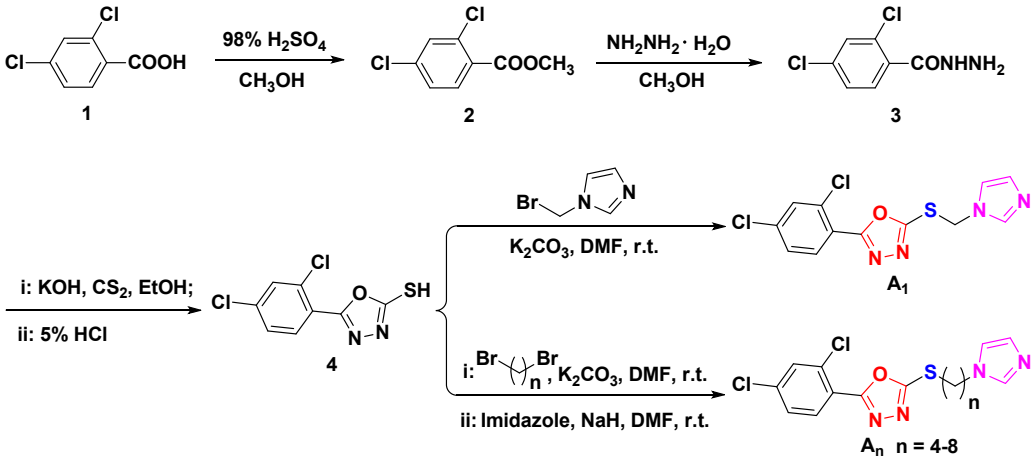

Scheme 1. Synthetic route for the target molecules $\mathbf{A_n}$ (n = 1, 4-8).

Table 1. Antibacterial activities of target compounds $\mathbf{A_n}$ against plant pathogens *Xoo* and *Xac in vitro*.

Compd.	*Xoo*			*Xac*		
	Regression equation	r	EC_{50} (μg/mL)	Regression equation	r	EC_{50} (μg/mL)
$\mathbf{A_1}$	y = 7.849x - 6.979	1.00	33.6 ± 4.1	y = 1.038x + 3.295	0.99	43.9 ± 6.1
$\mathbf{A_4}$	y = 10.972x - 5.944	0.98	9.94 ± 0.94	y = 1.473x + 3.898	0.98	5.60 ± 0.38
$\mathbf{A_5}$	y = 7.927x + 0.337	0.95	3.87 ± 0.10	y = 0.669x + 4.512	1.00	5.37 ± 0.81

A_6	y = 4.117x + 5.554	0.99	0.734 ± 0.122	y = 0.699x + 4.823	0.95	1.79 ± 0.15
A_7	y = 4.987x + 4.157	0.96	1.48 ± 0.08	y = 3.499x + 3.290	0.97	3.08 ± 0.05
A_8	y = 4.608x + 4.071	0.96	1.59 ± 0.01	y = 3.668x + 2.521	0.95	4.74 ± 0.05
BT	y = 1.499x + 2.052	0.98	92.6 ± 2.1	/	/	/
TC	y = 1.540x + 1.788	0.98	121.8 ± 3.6	y = 2.153x + 0.938	0.98	77.0 ± 2.0

312 Given that compound **A_6** exhibited excellent antibacterial potentials, we need to
313 clarify whether the modification of the crucial atoms would renovate the antibiotic
314 ability. Thus, the homologous intermediate **5** possessing a hydroxyl group instead of
315 the mercapto moiety and intermediate **6** suffering a 1,3,4-thiadiazole motif instead of
316 the 1,3,4-oxadiazole pattern were synthesized. Then two-step consecutive reactions
317 with dibromo-substituted alkyls and imidazole were carried out to afford the final
318 compounds **B_n** (n = 4–6, 8) and **C_n** (n = 4, 5, 8, 10). All the molecular structures were
319 confirmed by ^{1}H NMR, ^{13}C NMR, and HRMS (for detailed information, see
320 Supplementary data). As noted in Table 2, even fine-tuning crucial atoms had a
321 considerable influence toward bioactivity, illuminated by comparing the EC_{50} values
322 of **A_6** (0.734 and 1.79 μg/mL), **B_6** (5.35 and 7.37 μg/mL), and **C_6** (1.49 and 2.80
323 μg/mL). This finding suggested that the replacement of sulfur atom or
324 1,3,4-oxadiazole scaffold of **A_6** will weaken the interactions with bacterial receptors.
325 Similar patterns against *Xoo* were observable for compounds **B_n** and **C_n** providing the
326 EC_{50} values first decreasing and then increasing with tuning the alkyl lengths. This
327 finding further indicated that the balance of hydrophobicity/hydrophilicity of a
328 molecule is significant for the antimicrobial activity. Notably, compounds **B_n**
329 exhibited enhanced anti-*Xac* capacity with the increment of alkyl chain lengths and
330 afforded the minimal EC_{50} value of 3.05 μg/mL (n = 8, **B_8**). Similarly, for the series

331 **C_n**, the relatively best growth suppression against *Xac* was awarded for the molecule
332 **C_8** with EC_{50} value of 2.29 μg/mL. Significant decrement of antibacterial efficacy was
333 observed by approximately 41- and 5-fold against *Xoo* and *Xac* via switching the
334 1,3,4-oxadiazole ring (**A_6**, 0.734 and 1.79 μg/mL) into 4-amino-4*H*-1,2,4-triazole
335 motif (**D_6**, 30.3 and 8.92 μg/mL). Based on the above results, although bioactive
336 compounds were appreciably obtained, the antibacterial effect still not exceeded that
337 of compound **A_6**. This condition demonstrated that the 1,3,4-oxadiazole thioether was
338 favorable to the bioactivity.

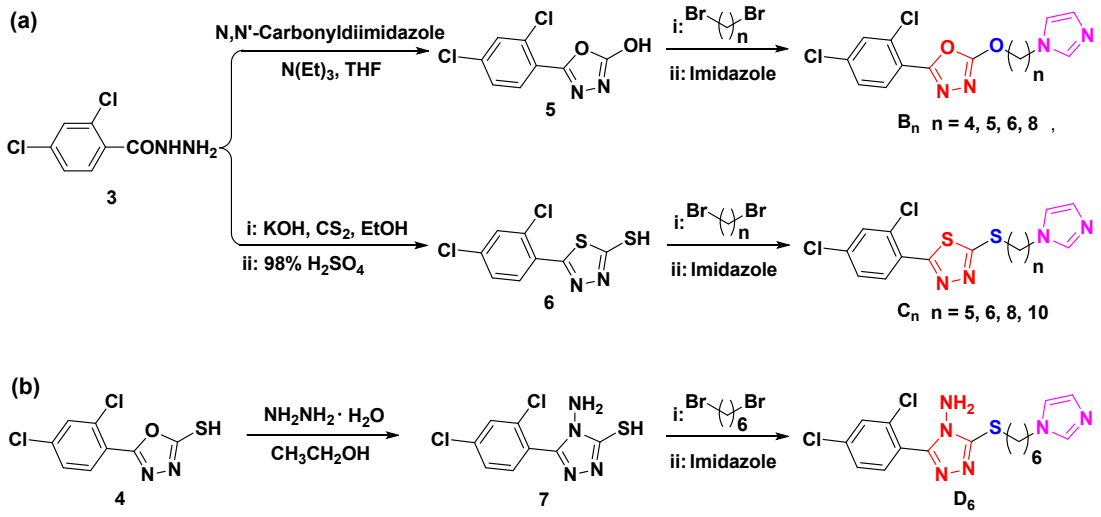

339

340 **Scheme 2.** Synthetic route for the target molecules: a) **B_n** and **C_n**; b) **D_6**.

341 **Table 2.** Antibacterial activities of target compounds **B_n**, **C_n**, and **D_6** against plant pathogens *Xoo* and *Xac in vitro*.

Compd.	*Xoo*			*Xac*		
	Regression equation	r	EC_{50} (μg/mL)	Regression equation	r	EC_{50} (μg/mL)
B_4	y = 11.199x - 10.590	0.99	24.6 ± 0.6	y = 7.106x - 3.938	0.93	24.9 ± 0.1
B_5	y = 9.023x - 2.549	1.00	6.87 ± 0.69	y = 6.750x - 1.109	0.95	8.03 ± 0.10
B_6	y = 8.425x - 1.139	0.92	5.35 ± 0.19	y = 6.466x - 0.609	0.97	7.37 ± 0.20
B_8	y = 23.429x - 12.688	1.00	5.69 ± 0.02	y = 2.684x + 3.700	0.98	3.05 ± 0.18
C_5	y = 5.274x + 3.589	0.95	1.85 ± 0.02	y = 6.466x + 1.979	0.97	2.93 ± 0.17
C_6	y = 2.837x + 5.408	0.93	1.49 ± 0.09	y = 0.828x + 4.6303	1.00	2.80 ± 0.71
C_8	y = 2.940x + 4.024	0.99	2.15 ± 0.07	y = 0.856x + 4.692	0.98	2.29 ± 0.31

C_{10}	y = 1.709x + 4.024	0.97	3.72 ± 0.29	y = 2.248x + 3.831	0.99	3.31 ± 0.08
D_6	y = 12.385x - 13.345	0.98	30.3 ± 3.3	y = 1.628x + 3.453	0.98	8.92 ± 1.42
BT	y = 1.499x + 2.052	0.98	92.6 ± 2.1	/	/	/
TC	y = 1.540x + 1.788	0.98	121.8 ± 3.6	y = 2.153x + 0.938	0.98	77.0 ± 2.0

From the above distilled result, we aimed to keep the (6-(1*H*-imidazol-1-yl)hexyl)thio at the 2-position of 1,3,4-oxadiazole and investigate the substituents on the 5-position of 1,3,4-oxadiazole toward bioactivity. The bioassay result (Table 3) revealed that antibacterial powers of these compounds were inordinately reduced after replacing the 2,4-dichlorophenyl into other fragments except compound **E_7** owning a phenyl group was discovered possessing the comparative anti-*Xac* bioactivity (2.02 μg/mL) with that of compound **A_6** (1.79 μg/mL). This phenomenon revealed that a providential substituent at the 5-position of 1,3,4-oxadiazole will promote and participate in several interactions targeting for the bacterial receptors. Evaluation of this data set enables preliminary structure-activity relationship to be defined for 5-substituted 1,3,4-oxadiazoles. Notably, the electronic effect of substituents on the benzene ring had a significant action in forecasting the anti-*Xoo* and anti-*Xac* activity, displayed by the comparison of EC_{50} values of compound **E_1** with a strong electron-withdrawing group (3-NO_2, 9.69 and 12.3 μg/mL), **E_5** with a weak electron-withdrawing halogen (3-Cl, 3.63 and 3.24 μg/mL), and **E_9** with a good electron-donating group (3-OCH_3, 10.1 and 6.29 μg/mL). Additionally, the substituent position on the benzene ring affected the activity, presenting similar patterns for the anti-*Xoo* and anti-*Xac* ability. The order of activities followed meta (R = 3-Cl, **E_5**, 3.63 and 3.24 μg/mL) > para (R = 4-Cl, **E_4**, 4.05 and 4.06 μg/mL) > ortho (R = 2-Cl, **E_6**, 4.47 and 6.36 μg/mL). The halogen type

362 also performed certain actions on bioactivity, illustrated by the view of EC_{50} values of
363 compounds **E_3** (R = 4-F, 9.43 and 5.59 μg/mL) and **E_4** (R = 4-Cl, 4.05 and 4.06
364 μg/mL). Clearly, the corresponding bioactivity against *Xoo* and *Xac* was significantly
365 knocked down by approximately 82- and 37-fold by changing 2,4-dichlorophenyl into
366 2-furyl. By contrast, acceptable antibiotic ability was achieved for compound **E_{11}**
367 decorating with a 3-pyridyl moiety and provided the EC_{50} values of 6.15 and 10.8
368 μg/mL against *Xoo* and *Xac*, respectively. Notably, the antibacterial potency toward
369 *Xoo* greatly decreased from 4.05 μg/mL (**E_4**) to 10.9 μg/mL (**E_{12}**) because of the
370 insertion of a hydrophobic methylene group between 4-chlorophenyl and
371 1,3,4-oxadiazole motifs. Meanwhile, the opposite pattern was obtained by inlaying an
372 oxymethylene group and resulted in ameliorative bioactivity from 7.73 μg/mL (**E_7**) to
373 6.13 μg/mL (**E_{13}**). Surprisingly, completely quenched antiseptic power was
374 observable as introducing a methyl group (**E_{14}**) at the 5-position of 1,3,4-oxadiazole.
375 This finding suggested that fragments with even large steric hindrance at 5-position
376 might be beneficial to the bioactivity. In view of the above studies, the antibacterial
377 competence can be shaken by a variety of factors including alkyl length of the tailor,
378 bridging atoms, electronic properties, the position of substituents, the type of halogen,
379 and steric hindrance of substituents. This phenomenon reminded us to elaborately
380 optimize the molecular structures.

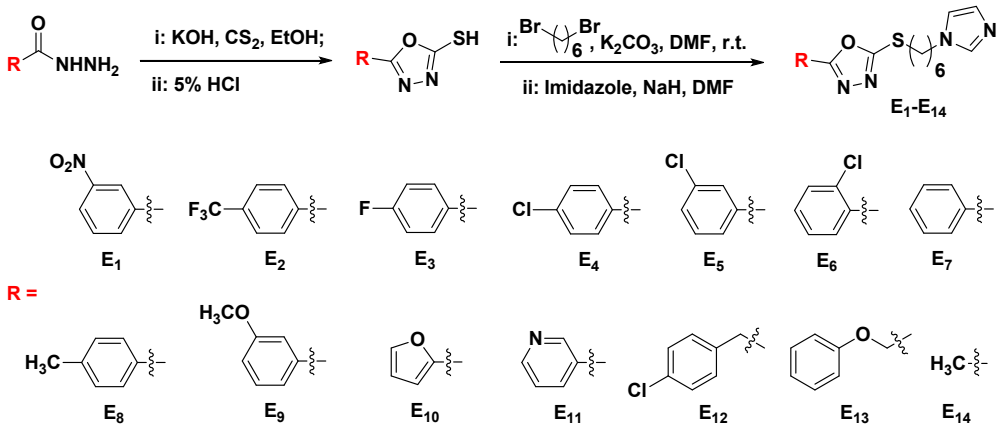

Scheme 3. Synthetic route for the target molecules **E_1-E_{14}**.

Table 3. Antibacterial activities of target compounds **E_1–E_{14}** against plant pathogens *Xoo* and *Xac in vitro*.

Compd.	*Xoo*			*Xac*		
	Regression equation	r	EC_{50} (μg/mL)	Regression equation	r	EC_{50} (μg/mL)
E_1	y = 5.839x - 0.760	0.97	9.69 ± 0.09	y = 1.256x + 3.633	0.96	12.3 ± 0.4
E_2	y = 6.101x + 1.796	0.98	3.35 ± 0.03	y = 2.643x + 3.289	0.99	4.44 ± 0.08
E_3	y = 9.975x - 4.720	0.97	9.43 ± 0.49	y = 1.451x + 3.916	0.99	5.59 ± 0.35
E_4	y = 9.207x - 0.594	0.93	4.05 ± 0.10	y = 3.205x + 3.051	0.99	4.06 ± 0.01
E_5	y = 10.893x - 1.101	0.92	3.63 ± 0.02	y = 1.722x + 4.121	0.98	3.24 ± 0.32
E_6	y = 9.499x - 1.767	0.94	4.47 ± 0.12	y = 5.617x + 0.486	0.93	6.36 ± 0.17
E_7	y = 2.117x + 3.120	0.96	7.73 ± 0.19	y = 1.585x + 4.515	0.95	2.02 ± 0.23
E_8	y = 4.972x + 1.632	0.96	4.76 ± 0.23	y = 1.157x + 4.049	1.00	6.64 ± 0.13
E_9	y = 12.937x - 8.006	0.99	10.1 ± 0.2	y = 1.032x + 4.175	1.00	6.29 ± 0.49
E_{10}	y = 2.603x + 0.359	1.00	60.7 ± 2.0	y = 3.749x – 1.857	0.99	67.4 ± 3.0
E_{11}	y = 3.938x + 1.893	1.00	6.15 ± 0.19	y = 3.291x + 1.603	0.98	10.8 ± 0.2
E_{12}	y = 13.028x - 8.512	1.00	10.9 ± 1.2	y = 0.587x + 4.721	1.00	7.99 ± 0.55
E_{13}	y = 3.680x + 2.101	0.99	6.13 ± 0.57	y = 1.776x + 3.676	0.98	5.56 ± 0.52
E_{14}	/	/	> 100	/	/	> 100
BT	y = 1.499x + 2.052	0.98	92.6 ± 2.1	/	/	/
TC	y = 1.540x + 1.788	0.98	121.8 ± 3.6	y = 2.153x + 0.938	0.98	77.0 ± 2.0

After the antibacterial performance of substituents on the 5-position of 1,3,4-oxadiazole had been evaluated, we need to clarify if the replacement of imidazole motif will renovate the antibacterial activity. Therefore,

387 5-(2,4-dichlorophenyl)-1,3,4-oxadiazoles bearing different imidazole analogs were
388 constructed. Bioassay results are shown in Table 4 and revealed that the bioactivity
389 can be dramatically revised by the type of imidazole analogs. Clearly, drastically
390 reduced antiseptic function was observable after switching the imidazole moiety into
391 1*H*-pyrazole (predicted pKa ≈ 2.27, **F_1**) or 1*H*-1,2,4-triazole (predicted pKa ≈ 3.30,
392 **F_2**) scaffolds. This condition indicated that the proton reception nature of imidazole
393 motif (predicted pKa ≈ 7.09, **A_6**) may probably strengthen or promote the several
394 interactions orientating for the cell receptors or target species. Conversely, tolerable
395 bioactivity was achieved for compound **F_3** bearing a 4-pyridinyloxy group (predicted
396 pKa ≈ 6.73) affording the EC_{50} values of 18.6 and 26.5 μg/mL against *Xoo* and *Xac*,
397 respectively. Compounds **F_4–F_6** offered frustrating growth inhibition effect toward
398 these two bacterial strains possibly ascribed to the large steric hindrance of these
399 fragments (nonplanar, whereas compound **A_6** provides a planar pattern for the
400 imidazole moiety) blocking the several interactions with bacterial receptors. Base on
401 the upon exploration, 2-((6-(1*H*-imidazol-1-yl)hexyl)thio)-5-(2,4-dichlorophenyl)-
402 1,3,4-oxadiazole (**A_6**) can serve as a new lead indicator in research on antibacterial
403 chemotherapy.

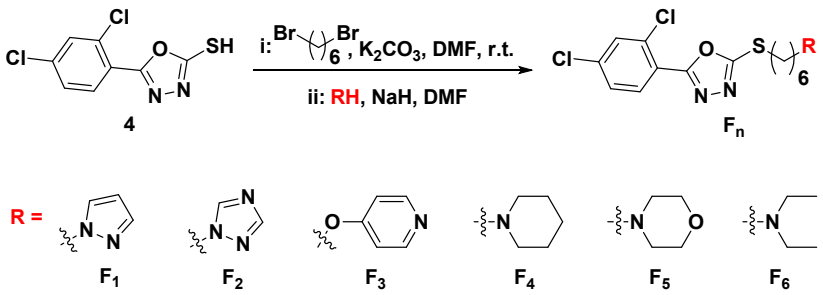

404

405 **Scheme 4.** Synthetic route for the target molecules **F_1–F_6**.

406 **Table 4.** Antibacterial activities of target compounds **F_1–F_6** against plant pathogens *Xoo* and *Xac in vitro*.

Compd.	*Xoo*			*Xac*		
	Regression equation	r	EC_{50} (μg/mL)	Regression equation	r	EC_{50} (μg/mL)
F_1	/	/	> 100	y = 1.388x + 2.380	0.99	77.2 ± 8.0
F_2	/	/	> 100	y = 2.827x + 0.281	1.00	46.7 ± 2.0
F_3	y = 6.847x - 3.685	0.99	18.6 ± 0.6	y = 2.127x + 1.974	0.99	26.5 ± 0.7
F_4	y = 2.583x + 0.395	0.96	60.6 ± 1.9	y = 0.757x + 4.136	0.93	13.8 ± 3.2
F_5	/	/	> 100	/	/	> 100
F_6	y = 2.302x + 1.054	1.00	51.8 ± 8.6	y = 1.561x + 3.087	0.97	16.2 ± 0.5
BT	y = 1.499x + 2.052	0.98	92.6 ± 2.1	/	/	/
TC	y = 1.540x + 1.788	0.98	121.8 ± 3.6	y = 2.153x + 0.938	0.98	77.0 ± 2.0

To continuously explore highly efficient structures based on the bioactive molecule **A_6**, the competent imidazolium scaffold was employed and integrated into the system to investigate the variation toward bioactivity. As shown in Scheme 5, the target compounds **G_1–G_{18}** can be obtained by the reactions of compound **A_6** with various alkyl halides, alkenyl halides, or substituted benzyl halides. Bioassay results declared that the effect of fusing the imidazolium group on potency was extremely apparent (Table 5) and provided admirable EC_{50} values ranging from 0.295 μg/mL to 2.92 μg/mL and 0.607 μg/mL to 2.99 μg/mL against *Xoo* and *Xac*, respectively. This finding suggested that the imidazolium scaffold can be considered an ideal and capable handle to renovate the antiseptic performance of target compounds. The homolog series **G_1–G_8** (from the methyl to octyl group) performed a trend of sharp increase on the antibacterial potency along with the extension of alkyl chain lengths and resulted in the minimum EC_{50} values of 0.295 and 0.611 μg/mL against *Xoo* and *Xac*, respectively. These values were quite better than those of **A_6**, **BT**, and **TC**. Notably, the comprehensive antibiotic ability of compounds **G_5-G_8** had already exceeded that of leading molecule **A_6**. Additionally, compound **G_9** bearing an allyl

group displayed permissible actions against *Xoo* and *Xac* with EC_{50} values of 1.42 and 2.70 μg/mL, respectively. The truth that compounds **G_{10}-G_{18}** decorating with substituted benzyl motifs paraded potent antibacterial competence toward plant pathogens which had outstripped that of **A_6** except compound **G_{14}** exerted slightly reduced capacity against *Xoo* with EC_{50} value of 0.885 μg/mL. This result demonstrated that coupling the key fragments of 1,3,4-oxadiazole skeleton and imidazolium nucleus in a single molecular architecture did elevate the power for attacking the bacterial resistance.

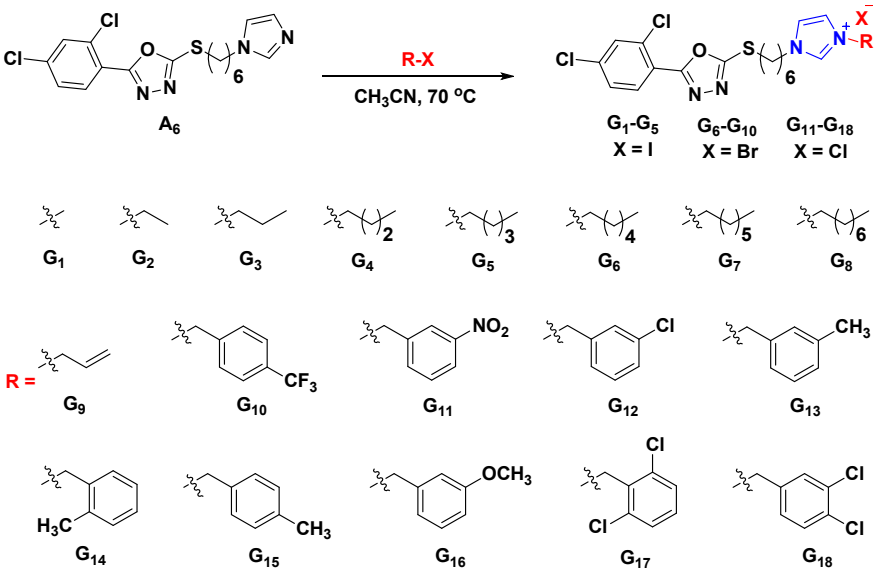

Scheme 5. Synthetic route for the target molecules **G_1–G_{18}**.

Table 5. Antibacterial activities of target compounds **G_1–G_{18}** against plant pathogens *Xoo* and *Xac in vitro*.

Compd.	*Xoo*			*Xac*		
	Regression equation	r	EC_{50} (μg/mL)	Regression equation	r	EC_{50} (μg/mL)
G_1	y = 2.060x + 4.040	0.99	2.92 ± 0.15	y = 1.058x + 4.497	0.99	2.99 ± 0.76
G_2	y = 2.710x + 3.961	0.99	2.42 ± 0.23	y = 0.977x + 4.861	0.99	1.39 ± 0.07
G_3	y = 2.271x + 4.074	0.96	2.56 ± 0.20	y = 0.886x + 4.974	0.98	1.07 ± 0.30
G_4	y = 0.898x + 4.686	0.98	2.24 ± 0.40	y = 0.867x + 5.085	0.98	0.799 ± 0.170
G_5	y = 4.672x + 5.800	0.97	0.674 ± 0.043	y = 2.448x + 5.446	0.96	0.658 ± 0.043
G_6	y = 4.496x + 6.971	0.95	0.364 ± 0.029	y = 4.225x + 5.140	0.99	0.927 ± 0.172

G_7	y = 3.858x + 5.703	0.97	0.657 ± 0.016	y = 2.107x + 4.806	0.94	1.24 ± 0.05
G_8	y = 4.609x + 7.442	0.95	0.295 ± 0.021	y = 4.447x + 5.950	0.99	0.611 ± 0.023
G_9	y = 1.506x + 4.768	0.97	1.42 ± 0.05	y = 1.251x + 4.453	0.98	2.70 ± 0.47
G_{10}	y = 3.925x + 6.043	0.97	0.542 ± 0.061	y = 4.327x + 4.416	0.98	1.36 ± 0.13
G_{11}	y = 7.162x + 7.874	0.99	0.397 ± 0.007	y = 9.123x + 3.297	1.00	1.54 ± 0.07
G_{12}	y = 3.659x + 5.930	0.95	0.557 ± 0.033	y = 0.818x + 5.043	0.98	0.886 ± 0.107
G_{13}	y = 4.674x + 6.528	0.98	0.471 ± 0.016	y = 5.501x + 6.192	0.98	0.607 ± 0.166
G_{14}	y = 5.479x + 5.290	0.99	0.885 ± 0.044	y = 3.426x + 4.787	0.99	1.15 ± 0.12
G_{15}	y = 3.563x + 6.891	0.98	0.295 ± 0.003	y = 5.094x + 5.534	0.99	0.786 ± 0.024
G_{16}	y = 3.438x + 6.445	0.99	0.380 ± 0.018	y = 3.202x + 5.138	1.00	0.906 ± 0.062
G_{17}	y = 4.677x + 6.624	0.98	0.449 ± 0.027	y = 4.810x + 4.053	1.00	1.57 ± 0.16
G_{18}	y = 4.442x + 6.824	1.00	0.389 ± 0.009	y = 3.174x + 5.611	0.95	0.642 ± 0.047
BT	y = 1.499x + 2.052	0.98	92.6 ± 2.1	/	/	/
TC	y = 1.540x + 1.788	0.98	121.8 ± 3.6	y = 2.153x + 0.938	0.98	77.0 ± 2.0

To explore the antibacterial action mechanism toward *Xoo* and *Xac*, SEM, TEM and FM were employed to investigate the morphology changes after treating with different concentrations of bioactive compounds **A_6** and **G_8** which were selected for this study. These compounds were nontoxic toward plants at the dosage of 200 μg/mL (Supporting information Figure Sa). A scene form SEM images manifested that the morphologies of *Xoo* were transformed from well-shaped (without treating with compounds **A_6** or **G_8**, Figures 2a and 2i, Figure Sb) to partially corrugated or broken after treating with 2×EC_{50}, 5×EC_{50}, and 25 μg/mL of compounds **A_6** or **G_8** (Figures 2b-2c and 2j-2k). This finding indicated that the designed compounds paraded the strong interactions with these plant pathogens. Further increasing the drug dosage to 50 μg/mL led to the appearance of abundant bacterial debris and leakage holes (Figures 2d and 2l). This phenomenon demonstrated that this type of compounds might master the privileged powers for attacking pathogens due to the proton

447 reception nature of imidazole motif and imidazolium cation part can promote the
448 interactions with the bacterial membrane. Similar patterns (Figures 2e-2h and 2i-2l,
449 Figure Sb) against *Xac* were observed before and after the addition of different
450 concentrations of designed compounds $\mathbf{A_6}$ or $\mathbf{G_8}$. Additionally, TEM images (Figure
451 Sc) of compounds $\mathbf{A_6}$ and $\mathbf{G_8}$ against *Xoo* and *Xac* at the drug concentrations of
452 $2\times EC_{50}$ and $5\times EC_{50}$ values further suggested that the rationally integrating key
453 fragments of 1,3,4-oxadiazole skeleton and imidazole (or imidazolium) nucleus in a
454 single molecule did display the competence to suppress and destroy the growth of
455 plant pathogenic bacteria. Propidium iodide (PI), a nonfluorescent dye, which can
456 form PI-DNA complex producing strong red fluorescence, is usually used to evaluate
457 cell permeability or viability but cannot cross the membrane of intact live bacteria.[45]
458 From confocal images (Figure Sd), the amount of red fluorescent bacteria gradually
459 increased with the improvement of concentration of compounds $\mathbf{A_6}$ or $\mathbf{G_8}$. This
460 finding indicated that the permeability of bacterial membrane was gradually enhanced
461 and resulted in the entrance of PI and the subsequent formation of PI–DNA complex
462 to produce fluorescence. An intriguing finding revealed that only compound $\mathbf{G_8}$
463 commanded another specific power to block the *Xoo* bipartition and resulted in the
464 observation of superlong bacteria (Figures 3a-3e). This condition suggested that
465 imidazolium-labeled 1,3,4-oxadiazole thioethers might target the filamentous
466 temperature-sensitive protein Z (FtsZ), which had been verified to play an important
467 role in cell division.[46] To date, the expression and purification of FtsZ protein are
468 ongoing, and further research for the interactions between imidazolium-labeled

469 1,3,4-oxadiazole thioethers and FtsZ protein will be presented in our coming work.

470

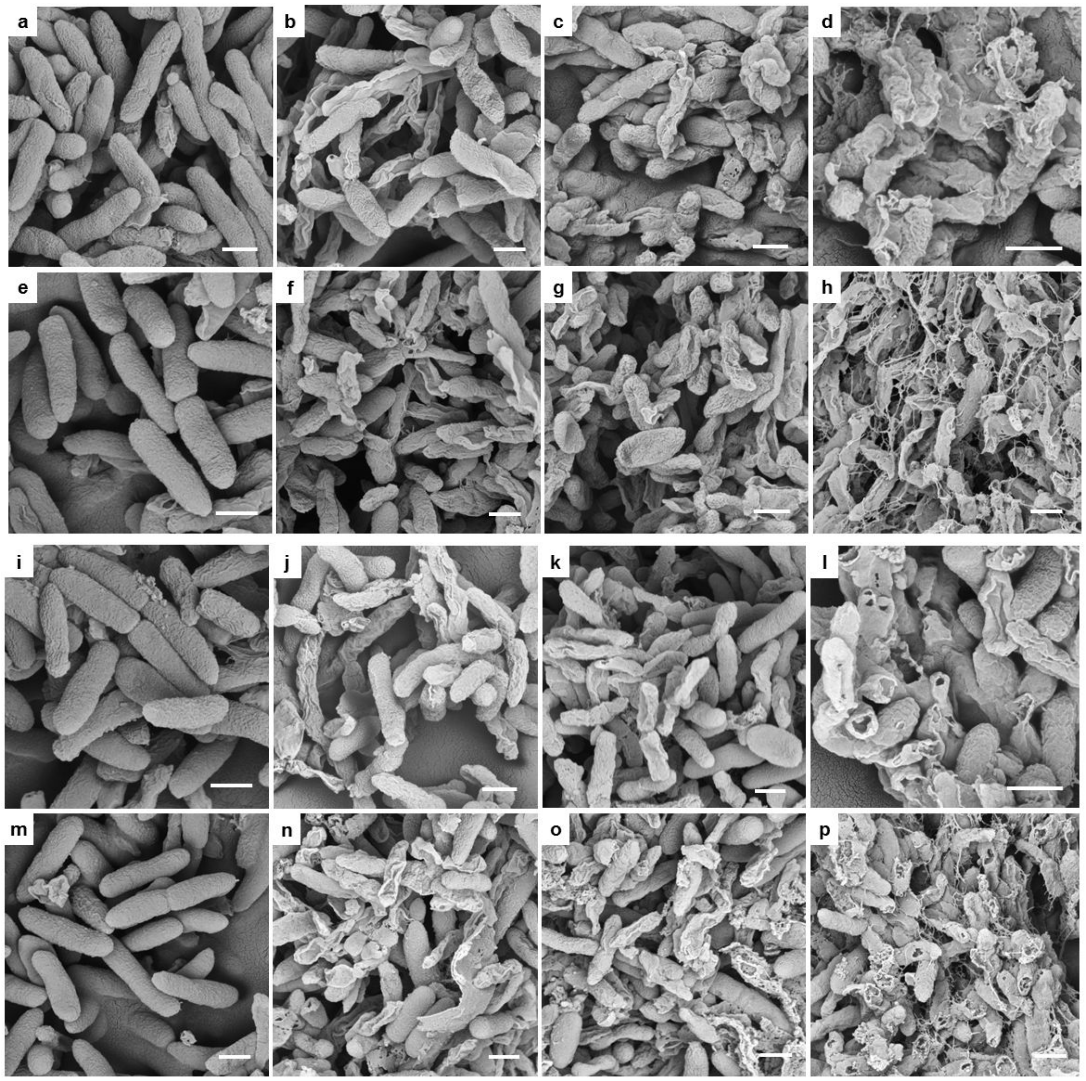

471

472 **Figure 2.** SEM images for *Xoo* and *Xac* after being incubated in different

473 concentrations of compound $\mathbf{A_6}$ and $\mathbf{G_8}$; $\mathbf{A_6}$: *Xoo* images for (a) 0 μg/mL, (b, c) 25

474 μg/mL, and (d) 50 μg/mL, *Xac* images for (e) 0 μg/mL, (f, g) 25 μg/mL, and (h) 50

475 μg/mL; $\mathbf{G_8}$: *Xoo* images for (i) 0 μg/mL, (j, k) 25 μg/mL, and (l) 50 μg/mL, *Xac*

476 images for (m) 0 μg/mL, (n, o) 25 μg/mL, and (p) 50 μg/mL. Scale bars for (a-p) are

477 500 nm.

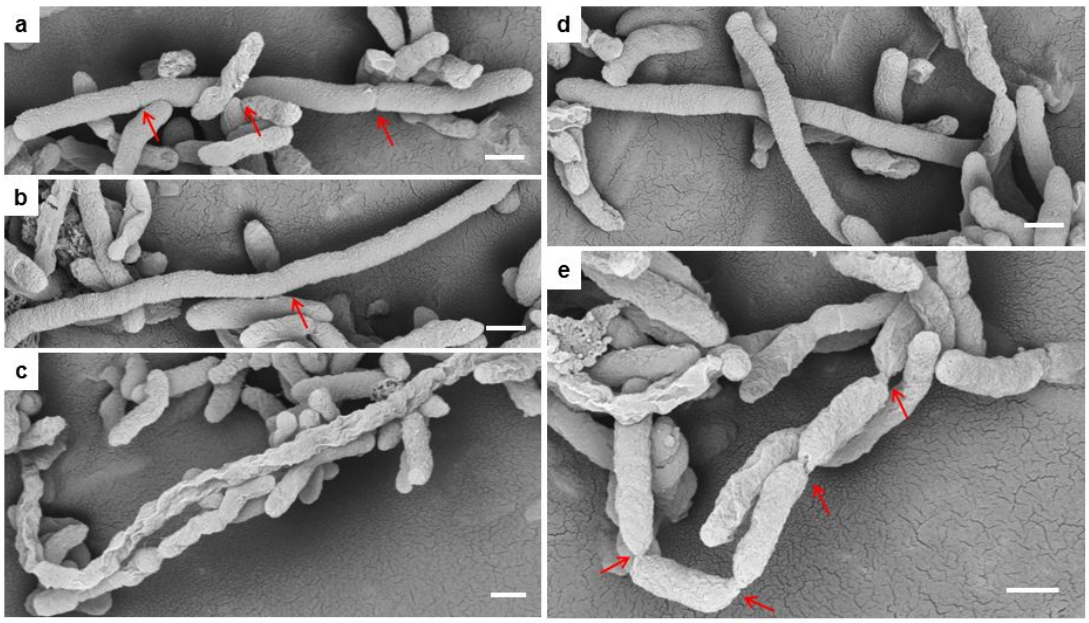

Figure 3. SEM images for *Xoo* after being incubated in 25 μg/mL of compound $\mathbf{G_8}$; scale bars for (a-e) are 500 nm.

In view of the above exploration and investigation, a plausible action mechanism for attacking pathogens of imidazole (or imidazolium)-labeled 1,3,4-oxadiazole thioethers was proposed. For the former (Figure 4A), first, a portion of the target molecules would be protonated due to the proton reception nature of imidazole motif. Consequently, these molecules carrying protonated imidazole and unprocessed imidazolium (for the later, Figure 4B) portions began to deposit via electrostatic interactions between cationic parts with anionic cell components (probably with both lipids and proteins). Meanwhile, some of them would enter inside by means of endocytosis, which tends to target the bacterial species. Then, the hydrophobic fragments would penetrate the bacterial membrane, leading to the disorganization of cell membranes and leakage of low-molecular-weight material. Finally, the bacterial cell wall components were destroyed probably by releasing autolytic enzymes and

consequently resulting in the leak of cellular components and bacterial death. Considering the simple molecular structures, easily synthetic procedure, and capable competence against pathogenic bacterium, imidazole (or imidazolium)-labeled 1,3,4-oxadiazole thioethers can be further developed as potential indicators against plant bacterial diseases.

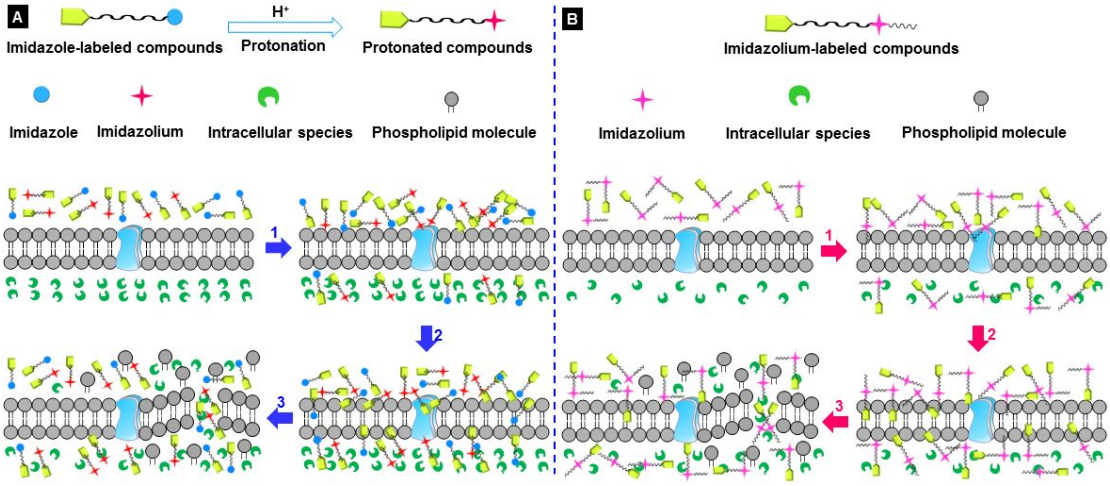

Figure 4. Proposed action mechanism for 1,3,4-oxadiazole thioethers bearing the imidazole groups (A) or imidazolium scaffolds (B) against plant pathogens.

Supporting Information

Supplementary data including characterization data for other target compounds. Figures Sa-Sd, and ^{1}H NMR, ^{19}F NMR, ^{13}C NMR, and HRMS spectra of all the compounds (Figure S1 to S162) associated with this article can be found, in the online version, at https://pubs.acs.org/journal/jafcau.

Funding Sources

We acknowledge the financial support of the Key Technologies R&D Program (2014BAD23B01), National Natural Science Foundation of China (21372052, 21662009, 21702037, 31860516), the Research Project of Ministry of Education of

China (20135201110005, 213033A), and Guizhou Provincial S&T Program ([2012]6012, LH [2017]7259, [2017]5788).

Conflicts of interests

The authors declare no competing financial interest.

Reference

(1) Le Dang, Q.; Kim, W. K.; Cuong, M. N.; Choi, Y. H.; Choi, G. J.; Jang, K. S.; Park, M. S.; Lim, C. H.; Ngoc, H. L.; Kim, J. C. Nematicidal and Antifungal Activities of Annonaceous Acetogenins from Annona squamosa against Various Plant Pathogens. *J. Agric. Food Chem*. **2011**, *59*, 11160-11167.

(2) Jian, W. L.; He, D. H.; Xi, P. G.; Li, X. W. Synthesis and Biological Evaluation of Novel Fluorine-Containing Stilbene Derivatives as Fungicidal Agents against Phytopathogenic Fungi. *J. Agric. Food Chem*. **2015**, *63*, 9963-9969.

(3) Pham, D. Q.; Ba, D. T.; Dao, N. T.; Choi, G. J.; Vu, T. T.; Kim, J. C.; Giang, T. P. L.; Vu, H. D.; Dang, Q, L. Antimicrobial efficacy of extracts and constituents fractionated from Rheum tanguticum Maxim. ex Balf. rhizomes against phytopathogenic fungi and bacteria. *Ind. Crop. Prod*. **2017**, *108*, 442-450.

(4) Hou, Z.; Zhu, L. F.; Yu, X. C.; Sun, M. Q.; Miao, F.; Zhou, L. Design, Synthesis, and Structure–Activity Relationship of New 2-Aryl-3, 4-dihydro-β-carbolin-2-ium Salts as Antifungal Agents. *J. Agric. Food Chem*. **2016**, *64*, 2847-2854.

(5) Liang, Y.; Yang, D. S.; Cui, J. H. A graphene oxide/silver nanoparticle composite as a novel agricultural antibacterial agent against Xanthomonas oryzae pv.

532 oryzae for crop disease management. *New. J. Chem*. **2017**, *41*, 13692-13699

533 (6) Wang, B.; Wu, G. C.; Zhang, Y. Q.; Qian, G. L.; Liu, F. Q. Dissecting the
534 virulence - related functionality and cellular transcription mechanism of a conserved
535 hypothetical protein in Xanthomonas oryzae pv. oryzae. *Mol. Plant. Pathol*. **2018**, *19*,
536 1859-1872.

537 (7) Li, P.; Hu, D. Y.; Xie, D. D.; Chen, J. X.; Jin, L. H.; Song, B. A. Design,
538 Synthesis, and Evaluation of New Sulfone Derivatives Containing a 1,3,4-Oxadiazole
539 Moiety as Active Antibacterial Agents. *J. Agric. Food Chem*. **2018**, *66*, 3093-3100.

540 (8) Yugander, A.; Sundaram, R. M.; Ladhalakshmi, D.; Hajira, S. K.; Prakasam,
541 V.; Prasad, M. S.; Madhav, M. S.; Babu, V. R.; Laha, G. S. Virulence profiling of
542 Xanthomonas oryzae pv. oryzae isolates, causing bacterial blight of rice in India. *Eur.*
543 *J. Plant. Pathol*. **2017**, *149*, 171-191.

544 (9) Ngo, H. P. T.; Ho, T. H.; Lee, I.; Tran, H. T.; Sur, B.; Kim, S.; Kim, J. G.;
545 Ahn, Y. J.; Cha, S. S.; Kang, L. W. Crystal Structures of Peptide Deformylase from
546 Rice Pathogen Xanthomonas oryzae pv. oryzae in Complex with Substrate Peptides,
547 Actinonin, and Fragment Chemical Compounds. *J. Agric. Food Chem*. **2016**, *64*,
548 7307-7314.

549 (10) Liang, X. Y.; Yu, X. Y.; Pan, X. Y.; Wu, J.; Duan, Y. B.; Wang, J. X.; Zhou,
550 M. G. A thiadiazole reduces the virulence of Xanthomonas oryzae pv. oryzae by
551 inhibiting the histidine utilization pathway and quorum sensing. *Mol. Plant. Pathol*.
552 **2018**, *19*, 116-128.

553 (11) Ference, C, M.; Gochez, A. M.; Behlau, F.; Wang, N.; Graham, J. H.; Jones,

554 J. B. Recent advances in the understanding of Xanthomonas citri ssp citri
555 pathogenesis and citrus canker disease management. *Mol. Plant. Pathol*. **2018**, *19*,
556 1302-1318.

557 (12) Mirzaei-Najafgholi, H.; Tarighi, S.; Golmohammadi, M.; Taheri, P. The
558 Effect of Citrus Essential Oils and Their Constituents on Growth of Xanthomonas
559 citri subsp citri. *Molecules* **2017**, *22*, DOI: 10.3390/molecules22040591.

560 (13) Cohen, S. P.; Liu, H. X.; Argues, C. T.; Pereira, A.; Cruz, C. V.; Verdier, V.;
561 Leach, J. E. RNA-Seq analysis reveals insight into enhanced rice Xa7-mediated
562 bacterial blight resistance at high temperature. *Plos. One* **2017**, *12*, DOI:
563 10.1371/journal.pone.0187625.

564 (14) Avila-Quezada, G. D.; Esquivel, J. F.; Silva-Rojas, H. V.; Leyva-Mir, S. G.;
565 Garcia-Avila, C. D.; Quezada-Salinas, A.; Noriega-Orozco, L.; Rivas-Valencia, P.;
566 Ojeda-Barrios, D.; Melgoza-Castillo, A. Emerging plant diseases under a changing
567 climate scenario: Threats to our global food supply. *Emir. J. Food Agr*. **2018**, *30*,
568 443-450.

569 (15) Pan, X. Y.; Xu, S.; Wu, J.; Luo, J. Y.; Duan, Y. B.; Wang, J. X.; Zhang, F.;
570 Zhou, M. G, Screening and characterization, of Xanthomonas oryzae pv. oryzae
571 strains with resistance to pheazine-1-carboxylic acid. *Pestic. Biochem. Phys*. **2018**,
572 *145*, 8-14.

573 (16) Song, X. P.; Li, P.; Li, M. W.; Yang, A. M.; Yu, L.; Luo, L. Z.; Hu, D. Y.;
574 Song, B. A. Synthesis and investigation of the antibacterial activity and action
575 mechanism of 1, 3, 4-oxadiazole thioether derivatives. *Pestic. Biochem. Phys*. **2018**,

576 *147*, 11-19.

577 (17) Wang, P. Y.; Zhou, L.; Zhou, J.; Wu, Z. B.; Xue, W.; Song, B. A.; Yong, S.
578 Synthesis and antibacterial activity of pyridinium-tailored
579 2,5-substituted-1,3,4-oxadiazole thioether/sulfoxide/sulfone derivatives. *Bioorg. Med.*
580 *Chem. Lett*. **2016**, *26*, 1214-1217.

581 (18) Li, P.; Tian, P. Y.; Chen, Y. Z.; Song, X. P.; Xue, W.; Jin, L. H.; Hu, D. Y.;
582 Yang, S.; Song, B. A. Novel bisthioether derivatives containing a 1,3,4-oxadiazole
583 moiety: design, synthesis, antibacterial and nematocidal activities. *Pest. Manag. Sci*.
584 **2018**, *74*, 844-852.

585 (19) Zhou, J.; Tao, Q. Q.; Wang, P. Y.; Shao, W. B.; Wu, Z. B.; Li, Z.; Yang, S.
586 Antimicrobial evaluation and action mechanism of pyridinium-decorated
587 1,4-pentadien-3-one derivatives. *Bioorg. Med. Chem. Lett*. **2018**, *28*, 1742-1746.

588 (20) Chen, L.; Wang, P. Y.; Li, Z. X.; Zhou, L.; Wu, Z. B.; Song, B. A.; Yang, S.
589 Antiviral and Antibacterial Activities of N-(4-Substituted phenyl) Acetamide
590 Derivatives Bearing 1,3,4-Oxadiazole Moiety. *Chinese J. Chem*. **2016**, *34*, 1236-1244

591 (21) Su, X. L.; Xu, S.; Shan, Y.; Yin, M.; Chen, Y.; Feng, X.; Wang, Q. Z. Three
592 new quinazolines from Evodia rutaecarpa and their biological activity. *Fitoterapia*
593 **2018**, *127*, 186-192.

594 (22) Tu, H.; Wu, S. Q.; Li, X. Q.; Wan, Z. C.; Wan, J. L.; Tian, K.; Ouyang, G. P.
595 Synthesis and Antibacterial Activity of Novel 1H-indol-2-ol Derivatives. *J.*
596 *Heterocyclic. Chem*. **2018**, *55*, 269-275.

597 (23) Yao, W. R.; Wang, H. Y.; Wang, S. T.; Sun, S. L.; Zhou, J.; Luan, Y. Y.

598 Assessment of the Antibacterial Activity and the Antidiarrheal Function of Flavonoids
599 from Bayberry Fruit. *J. Agric. Food Chem*. **2011**, *59*, 5312-5317.
600 (24) Khalilullah, H.; Khan, S.; Nomani, M. S.; Ahmed, B. Synthesis,
601 characterization and antimicrobial activity of benzodioxane ring containing
602 1,3,4-oxadiazole derivatives. *Arab. J. Chem*. **2016**, *9*, S1029-S1035.
603 (25) Cui, Z. N.; Shi, Y. X.; Zhang, L.; Ling, Y.; Li, B. J.; Nishida, Y.; Yang, X. L.
604 Synthesis and Fungicidal Activity of Novel 2,5-Disubstituted-1,3,4-oxadiazole
605 Derivatives. *J. Agric. Food Chem*. **2012**, *60*, 11649-11656.
606 (26) Barot, K. P.; Manna, K. S.; Ghate, M. D. Design, synthesis and antimicrobial
607 activities of some novel 1,3,4-thiadiazole, 1,2,4-triazole-5-thione and
608 1,3-thiazolan-4-one derivatives of benzimidazole. *J. Saudi Chem. Soc*. **2017**, *21*,
609 S35-S43.
610 (27) Xu, W. M.; Han, F. F.; He, M.; Hu, D. Y.; He, J.; Yang, S.; Song, B. A.
611 Inhibition of tobacco bacterial wilt with sulfone derivatives containing an
612 1,3,4-oxadiazole moiety. *J. Agric. Food Chem*. **2012**, *60*, 1036-1041.
613 (28) Bondock, S.; Adel, S.; Etman, H. A.; Badria, F. A. Synthesis and antitumor
614 evaluation of some new 1,3,4-oxadiazole-based heterocycles. *Eur. J. Med. Chem*.
615 **2012**, *48*, 192-199.
616 (29) Behalo, M. S. An efficient one-pot catalyzed synthesis of
617 2,5-disubstituted-1,3,4-oxadiazoles and evaluation of their antimicrobial activities.
618 *RSC Adv*. *2016*, *6*, 103132-103136.
619 (30) Banerjee, A. G.; Das, N.; Shengule, S. A.; Srivastava, R. S.; Shrivastava, S.

620 K. Synthesis, characterization, evaluation and molecular dynamics studies of 5,
621 6-diphenyl-1,2,4 triazin-3(2H)-one derivatives bearing 5-substituted 1,3,4-oxadiazole
622 as potential anti-inflammatory and analgesic agents. *Eur. J. Med. Chem*. **2015**. *101*,
623 81-95.

624 (31) Chen, H. S.; Li, Z. M.; Han, Y. F. Synthesis and fungicidal activity against
625 Rhizoctonia solani of 2-alkyl (Alkylthio)-5-pyrazolyl-1,3,4-oxadiazoles
626 (Thiadiazoles). *J. Agric. Food Chem*. **2000**, *48*, 5312-5315.

627 (32) Zhou, L.; Wang, P. Y.; Zhou, J.; Shao, W. B.; Fang, H. S.; Wu, Z. B.; Yang,
628 S. Antimicrobial activities of pyridinium-tailored pyrazoles bearing 1,3,4-oxadiazole
629 scaffolds. *J. Saudi Chem. Soc*. **2017**, *21*, 852-860.

630 (33) Zou, X. J.; Lai, L. H.; Jin, G. Y.; Zhang, Z. X. Synthesis, fungicidal activity,
631 and 3D-QSAR of pyridazinone-substituted 1, 3, 4-oxadiazoles and 1, 3,
632 4-thiadiazoles. *J. Agric. Food Chem*. **2002**, *50*, 3757-3760.

633 (34) Duan, Y. T.; Wang, Z. C.; Sang, Y. L.; Tao, X. X.; Zhu, H. L. Exploration of
634 Structure-Based on Imidazole Core as Antibacterial Agents. *Curr. Top. Med. Chem*.
635 **2013**, *13*, 3118-3130.

636 (35) Li, W. J.; Li, Q.; Liu, D. Li.; Ding, M. W. Synthesis, Fungicidal Activity, and
637 Sterol 14α-Demethylase BindingInteraction of 2-Azolyl-3,4-dihydroquinazolines on
638 Penicillium digitatum. *J. Agric. Food Chem*. **2013**, *61*, 1419-1426.

639 (36) Chen, L.; Zhao, B.; Fan, Z. J; Liu, X. M.; Wu, Q. F.; Li, H. P.; Wang, H. X.
640 Synthesis of Novel 3,4-Chloroisothiazole-Based Imidazoles as Fungicides and
641 Evaluation of Their Mode of Action. *J. Agric. Food Chem*. **2018**, *66*, 7319-7327.

642 (37) Rani, N.; Sharma, A.; Singh, R. Imidazoles as Promising Scaffolds for
643 Antibacterial Activity: A Review. *Mini-Rev. Med. Chem*. **2013**, *13*, 1812-1835.
644 (38) Hu, Y.; Shen, Y. F.; Wu, X. H.; Tu, X.; Wang, G. X. Synthesis and
645 biological evaluation of coumarin derivatives containing imidazole skeleton as
646 potential antibacterial agents. *Eur. J Med. Chem*. **2018**, *143*, 958-969.
647 (39) Zheng, Z. Q.; Xu, Q. M.; Guo, J. N.; Qin, J.; Mao, H. L.; Wang, B.; Yan, F.
648 Structure-Antibacterial Activity Relationships of Imidazolium-Type Ionic Liquid
649 Monomers, Poly(ionic liquids) and Poly(ionic liquid) Membranes: Effect of Alkyl
650 Chain Length and Cations. *ACS Appl. Mater. Inter*. **2016**, *8*, 12684-12692.
651 (40) Wang, D.; Richter, C.; Ruhling, A.; Drucker, P.; Siegmund, D.;
652 Metzler-Nolte, N.; Glorius, F.; Galla, H. J. A Remarkably Simple Class of
653 Imidazolium-Based Lipids and Their Biological Properties. *Chem. Eur. J.* **2015**, *21*,
654 15123-15126.
655 (41) Borkowski, A.; Lawniczak, L.; Clapa, T.; Narcdna, D.; Selwet, M.; Peziak,
656 D.; Markiewicz, B.; Chrzanowski, L. Different antibacterial activity of novel
657 theophylline-based ionic liquids - Growth kinetic and cytotoxicity studies. *Ecotox.*
658 *Environ. Safe* **2016**, *130*, 54-64.
659 (42) Ganapathi, P.; Ganesan, K.; Vijaykanth, N.; Arunagirinathan, N.
660 Anti-bacterial screening of water soluble carbonyl diimidazolium salts and its
661 derivatives. *J. Mol. Liq*. **2016**, *219*, 180-185.
662 (43) Lee, S.; Cheng, H.; Chi, M.; Xu, Q.; Chen, X.; Eom, C. Y.; James, T. D.;
663 Park, S.; Yoon, J. Sensing and antibacterial activity of imidazolium-based conjugated

664 polydiacetylenes. *Biosens. Bioelectron*. **2016**, *77*, 1016-1019.

665 (44) Shamshina, J. L.; Kelley, S. P.; Gurau, G.; Rogers, R. D. Chemistry: Develop

666 ionic liquid drugs. *Nature News* **2015**, *528*, 188-189.

667 (45) Wang, J. F.; Chen, Y. P.; Yao, K. J.; Wilbon, P. A.; Zhang, W. J; Ren, L. X.;

668 Zhou, J. H.; Nagarkatti, M.; Wang, C. P.; Chu, F. X.; He, X. M.; Decho, A. W.; Tang,

669 C. B. Robust antimicrobial compounds and polymers derived from natural resin acids.

670 *Chem. Commun.* **2012**, *48*, 916-918.

671 (46) Haranahalli, K.; Tong, S.; Ojima, I. Recent advances in the discovery and

672 development of antibacterial agents targeting the cell-division protein FtsZ. *Bioorg.*

673 *Med. Chem.* **2016**, *24*, 6354-6369.

674

675 **Figures and Tables**

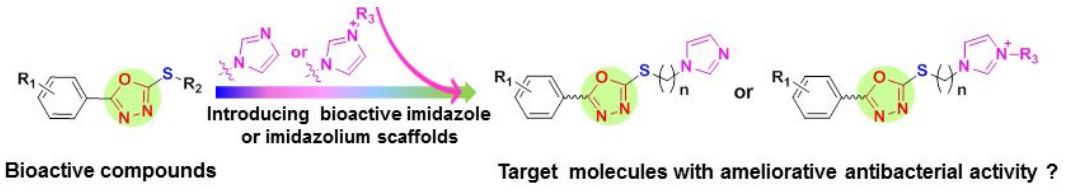

676

677 **Figure 1.** Design strategy for the target molecules.

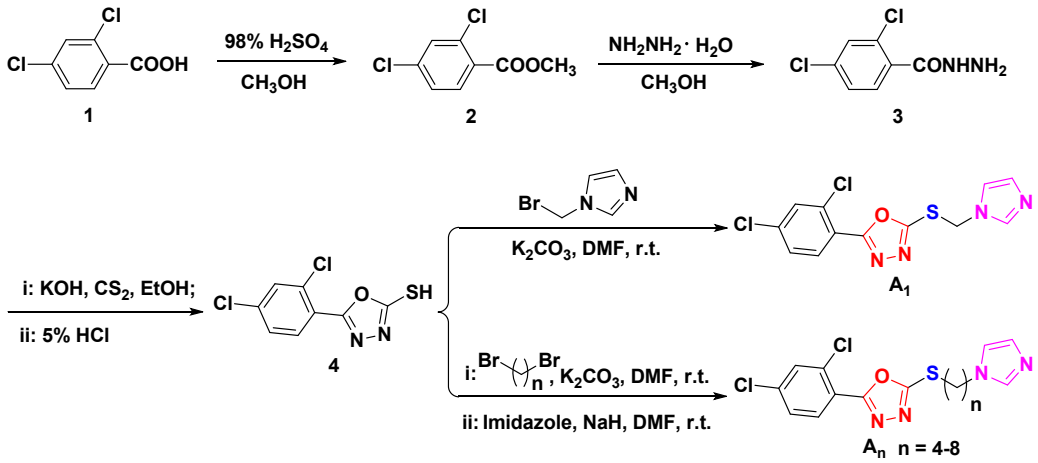

678

679 **Scheme 1.** Synthetic route for the target molecules $\mathbf{A_n}$ (n = 1, 4-8).

Table 1. Antibacterial activities of target compounds $\mathbf{A_n}$ against plant pathogen *Xoo* and *Xac in vitro*.

Compd.	*Xoo*			*Xac*		
	Regression equation	r	EC_{50} (μg/mL)	Regression equation	r	EC_{50} (μg/mL)
$\mathbf{A_1}$	y = 7.849x - 6.979	1.00	33.6 ± 4.1	y = 1.038x + 3.295	0.99	43.9 ± 6.1
$\mathbf{A_4}$	y = 10.972x - 5.944	0.98	9.94 ± 0.94	y = 1.473x + 3.898	0.98	5.60 ± 0.38
$\mathbf{A_5}$	y = 7.927x + 0.337	0.95	3.87 ± 0.10	y = 0.669x + 4.512	1.00	5.37 ± 0.81
$\mathbf{A_6}$	y = 4.117x + 5.554	0.99	0.734 ± 0.122	y = 0.699x + 4.823	0.95	1.79 ± 0.15
$\mathbf{A_7}$	y = 4.987x + 4.157	0.96	1.48 ± 0.08	y = 3.499x + 3.290	0.97	3.08 ± 0.05
$\mathbf{A_8}$	y = 4.608x + 4.071	0.96	1.59 ± 0.01	y = 3.668x + 2.521	0.95	4.74 ± 0.05
BT	y = 1.499x + 2.052	0.98	92.6 ± 2.1	/	/	/
TC	y = 1.540x + 1.788	0.98	121.8 ± 3.6	y = 2.153x + 0.938	0.98	77.0 ± 2.0

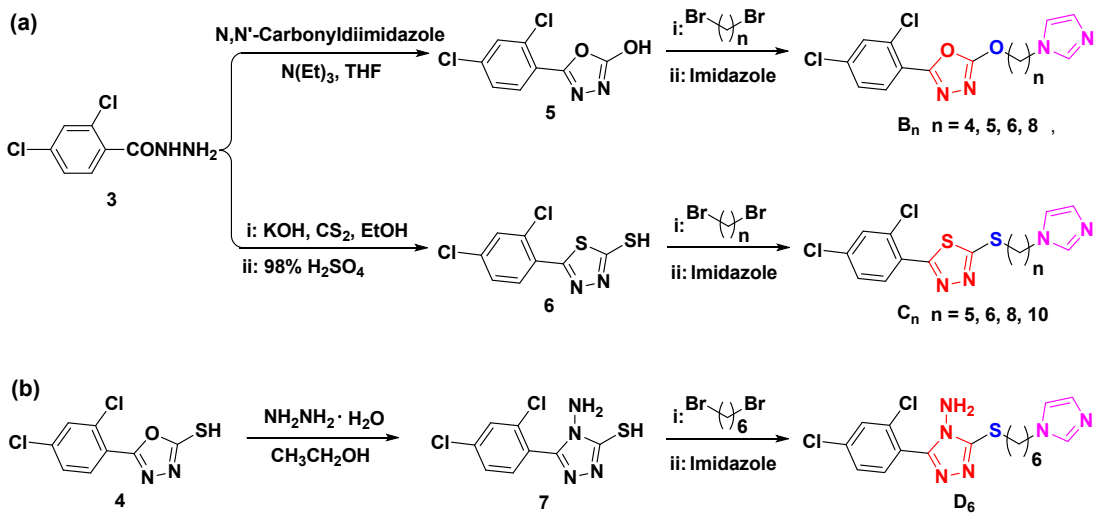

Scheme 2. Synthetic route for the target molecules: a) $\mathbf{B_n}$ and $\mathbf{C_n}$; b) $\mathbf{D_6}$.

Table 2. Antibacterial activities of target compounds $\mathbf{B_n}$, $\mathbf{C_n}$, and $\mathbf{D_6}$ against plant pathogens *Xoo* and *Xac in vitro*.

Compd.	*Xoo*			*Xac*		
	Regression equation	r	EC_{50} (μg/mL)	Regression equation	r	EC_{50} (μg/mL)
$\mathbf{B_4}$	y = 11.199x - 10.590	0.99	24.6 ± 0.6	y = 7.106x - 3.938	0.93	24.9 ± 0.1
$\mathbf{B_5}$	y = 9.023x - 2.549	1.00	6.87 ± 0.69	y = 6.750x - 1.109	0.95	8.03 ± 0.10
$\mathbf{B_6}$	y = 8.425x - 1.139	0.92	5.35 ± 0.19	y = 6.466x - 0.609	0.97	7.37 ± 0.20
$\mathbf{B_8}$	y = 23.429x - 12.688	1.00	5.69 ± 0.02	y = 2.684x + 3.700	0.98	3.05 ± 0.18
$\mathbf{C_5}$	y = 5.274x + 3.589	0.95	1.85 ± 0.02	y = 6.466x + 1.979	0.97	2.93 ± 0.17
$\mathbf{C_6}$	y = 2.837x + 5.408	0.93	1.49 ± 0.09	y = 0.828x + 4.6303	1.00	2.80 ± 0.71

C_8	y = 2.940x + 4.024	0.99	2.15 ± 0.07	y = 0.856x + 4.692	0.98	2.29 ± 0.31
C_{10}	y = 1.709x + 4.024	0.97	3.72 ± 0.29	y = 2.248x + 3.831	0.99	3.31 ± 0.08
D_6	y = 12.385x - 13.345	0.98	30.3 ± 3.3	y = 1.628x + 3.453	0.98	8.92 ± 1.42
BT	y = 1.499x + 2.052	0.98	92.6 ± 2.1	/	/	/
TC	y = 1.540x + 1.788	0.98	121.8 ± 3.6	y = 2.153x + 0.938	0.98	77.0 ± 2.0

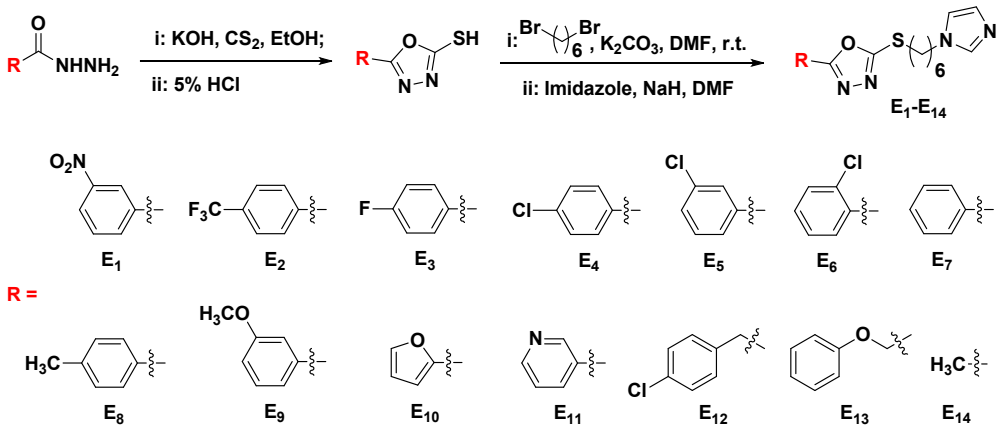

Scheme 3. Synthetic route for the target molecules **E_1-E_{14}**.

Table 3. Antibacterial activities of target compounds **E_1–E_{14}** against plant pathogens *Xoo* and *Xac in vitro*.

Compd.	*Xoo*			*Xac*		
	Regression equation	r	EC_{50} (μg/mL)	Regression equation	r	EC_{50} (μg/mL)
E_1	y = 5.839x - 0.760	0.97	9.69 ± 0.09	y = 1.256x + 3.633	0.96	12.3 ± 0.4
E_2	y = 6.101x + 1.796	0.98	3.35 ± 0.03	y = 2.643x + 3.289	0.99	4.44 ± 0.08
E_3	y = 9.975x - 4.720	0.97	9.43 ± 0.49	y = 1.451x + 3.916	0.99	5.59 ± 0.35
E_4	y = 9.207x - 0.594	0.93	4.05 ± 0.10	y = 3.205x + 3.051	0.99	4.06 ± 0.01
E_5	y = 10.893x - 1.101	0.92	3.63 ± 0.02	y = 1.722x + 4.121	0.98	3.24 ± 0.32
E_6	y = 9.499x - 1.767	0.94	4.47 ± 0.12	y = 5.617x + 0.486	0.93	6.36 ± 0.17
E_7	y = 2.117x + 3.120	0.96	7.73 ± 0.19	y = 1.585x + 4.515	0.95	2.02 ± 0.23
E_8	y = 4.972x + 1.632	0.96	4.76 ± 0.23	y = 1.157x + 4.049	1.00	6.64 ± 0.13
E_9	y = 12.937x - 8.006	0.99	10.1 ± 0.2	y = 1.032x + 4.175	1.00	6.29 ± 0.49
E_{10}	y = 2.603x + 0.359	1.00	60.7 ± 2.0	y = 3.749x – 1.857	0.99	67.4 ± 3.0
E_{11}	y = 3.938x + 1.893	1.00	6.15 ± 0.19	y = 3.291x + 1.603	0.98	10.8 ± 0.2
E_{12}	y = 13.028x - 8.512	1.00	10.9 ± 1.2	y = 0.587x + 4.721	1.00	7.99 ± 0.55
E_{13}	y = 3.680x + 2.101	0.99	6.13 ± 0.57	y = 1.776x + 3.676	0.98	5.56 ± 0.52
E_{14}	/	/	> 100	/	/	> 100

BT	y = 1.499x + 2.052	0.98	92.6 ± 2.1	/	/	/
TC	y = 1.540x + 1.788	0.98	121.8 ± 3.6	y = 2.153x + 0.938	0.98	77.0 ± 2.0

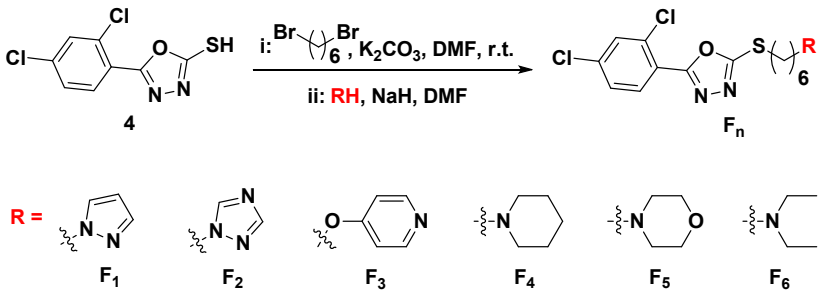

Scheme 4. Synthetic route for the target molecules $\mathbf{F_1}$–$\mathbf{F_6}$.

Table 4. Antibacterial activities of target compounds $\mathbf{F_1}$–$\mathbf{F_6}$ against plant pathogens *Xoo* and *Xac in vitro*.

Compd.	*Xoo*			*Xac*		
	Regression equation	r	EC_{50} (μg/mL)	Regression equation	r	EC_{50} (μg/mL)
$\mathbf{F_1}$	/	/	> 100	y = 1.388x + 2.380	0.99	77.2 ± 8.0
$\mathbf{F_2}$	/	/	> 100	y = 2.827x + 0.281	1.00	46.7 ± 2.0
$\mathbf{F_3}$	y = 6.847x - 3.685	0.99	18.6 ± 0.6	y = 2.127x + 1.974	0.99	26.5 ± 0.7
$\mathbf{F_4}$	y = 2.583x + 0.395	0.96	60.6 ± 1.9	y = 0.757x + 4.136	0.93	13.8 ± 3.2
$\mathbf{F_5}$	/	/	> 100	/	/	> 100
$\mathbf{F_6}$	y = 2.302x + 1.054	1.00	51.8 ± 8.6	y = 1.561x + 3.087	0.97	16.2 ± 0.5
BT	y = 1.499x + 2.052	0.98	92.6 ± 2.1	/	/	/
TC	y = 1.540x + 1.788	0.98	121.8 ± 3.6	y = 2.153x + 0.938	0.98	77.0 ± 2.0

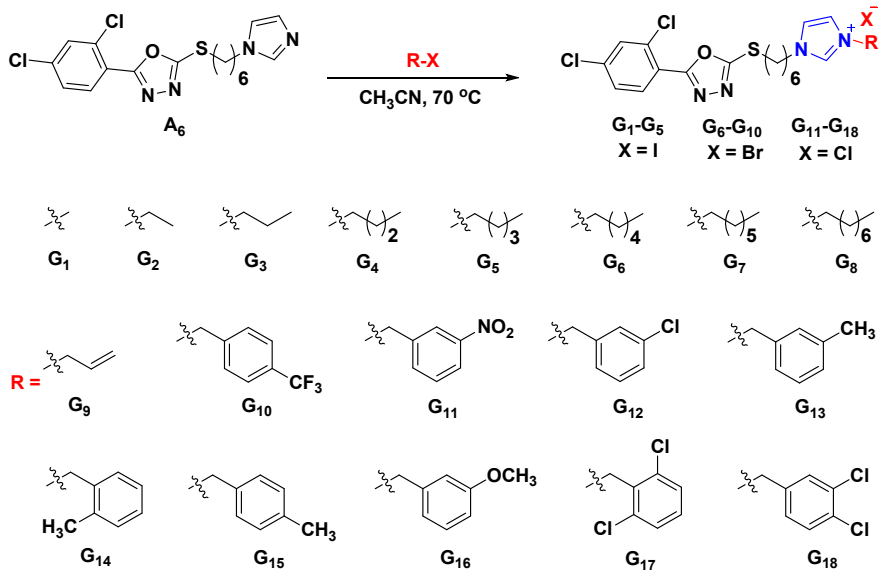

695 **Scheme 5.** Synthetic route for the target molecules **G_1–G_{18}**.

696 **Table 5.** Antibacterial activities of target compounds **G_1–G_{18}** against plant pathogens *Xoo* and *Xac in vitro*.

Compd.	*Xoo*			*Xac*		
	Regression equation	r	EC_{50} (μg/mL)	Regression equation	r	EC_{50} (μg/mL)
G_1	y = 2.060x + 4.040	0.99	2.92 ± 0.15	y = 1.058x + 4.497	0.99	2.99 ± 0.76
G_2	y = 2.710x + 3.961	0.99	2.42 ± 0.23	y = 0.977x + 4.861	0.99	1.39 ± 0.07
G_3	y = 2.271x + 4.074	0.96	2.56 ± 0.20	y = 0.886x + 4.974	0.98	1.07 ± 0.30
G_4	y = 0.898x + 4.686	0.98	2.24 ± 0.40	y = 0.867x + 5.085	0.98	0.799 ± 0.170
G_5	y = 4.672x + 5.800	0.97	0.674 ± 0.043	y = 2.448x + 5.446	0.96	0.658 ± 0.043
G_6	y = 4.496x + 6.971	0.95	0.364 ± 0.029	y = 4.225x + 5.140	0.99	0.927 ± 0.172
G_7	y = 3.858x + 5.703	0.97	0.657 ± 0.016	y = 2.107x + 4.806	0.94	1.24 ± 0.05
G_8	y = 4.609x + 7.442	0.95	0.295 ± 0.021	y = 4.447x + 5.950	0.99	0.611 ± 0.023
G_9	y = 1.506x + 4.768	0.97	1.42 ± 0.05	y = 1.251x + 4.453	0.98	2.70 ± 0.47
G_{10}	y = 3.925x + 6.043	0.97	0.542 ± 0.061	y = 4.327x + 4.416	0.98	1.36 ± 0.13
G_{11}	y = 7.162x + 7.874	0.99	0.397 ± 0.007	y = 9.123x + 3.297	1.00	1.54 ± 0.07
G_{12}	y = 3.659x + 5.930	0.95	0.557 ± 0.033	y = 0.818x + 5.043	0.98	0.886 ± 0.107
G_{13}	y = 4.674x + 6.528	0.98	0.471 ± 0.016	y = 5.501x + 6.192	0.98	0.607 ± 0.166
G_{14}	y = 5.479x + 5.290	0.99	0.885 ± 0.044	y = 3.426x + 4.787	0.99	1.15 ± 0.12
G_{15}	y = 3.563x + 6.891	0.98	0.295 ± 0.003	y = 5.094x + 5.534	0.99	0.786 ± 0.024
G_{16}	y = 3.438x + 6.445	0.99	0.380 ± 0.018	y = 3.202x + 5.138	1.00	0.906 ± 0.062
G_{17}	y = 4.677x + 6.624	0.98	0.449 ± 0.027	y = 4.810x + 4.053	1.00	1.57 ± 0.16
G_{18}	y = 4.442x + 6.824	1.00	0.389 ± 0.009	y = 3.174x + 5.611	0.95	0.642 ± 0.047
BT	y = 1.499x + 2.052	0.98	92.6 ± 2.1	/	/	/
TC	y = 1.540x + 1.788	0.98	121.8 ± 3.6	y = 2.153x + 0.938	0.98	77.0 ± 2.0

697

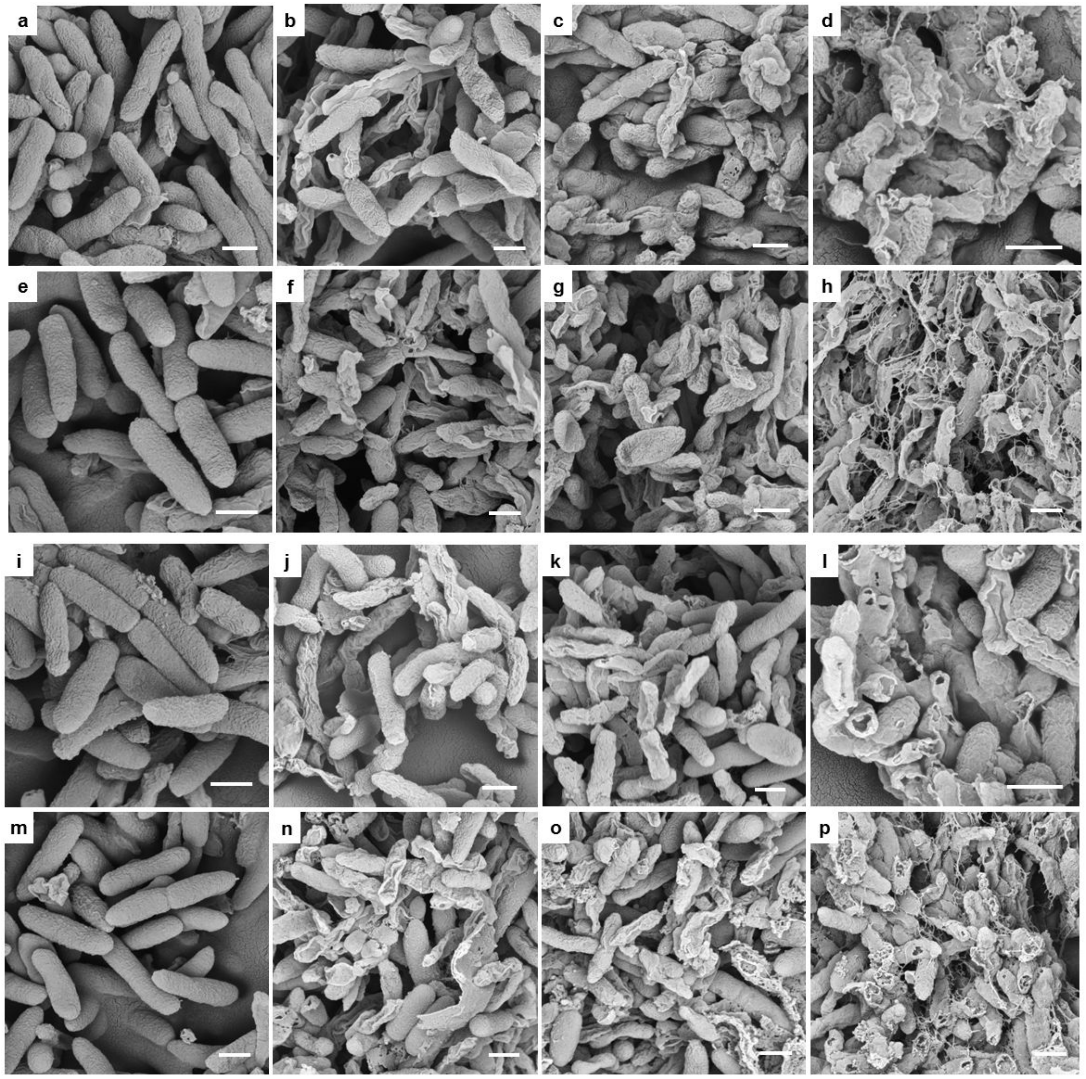

Figure 2. SEM images for *Xoo* and *Xac* after incubated in different concentration of compound $\mathbf{A_6}$ and $\mathbf{G_8}$; $\mathbf{A_6}$: *Xoo* images for (a) 0 μg/mL, (b, c) 25 μg/mL, and (d) 50 μg/mL, *Xac* images for (e) 0 μg/mL, (f, g) 25 μg/mL, and (h) 50 μg/mL; $\mathbf{G_8}$: *Xoo* images for (i) 0 μg/mL, (j, k) 25 μg/mL, and (l) 50 μg/mL, *Xac* images for (m) 0 μg/mL, (n, o) 25 μg/mL, and (p) 50 μg/mL. Scale bars for (a-p) are 500 nm.

705

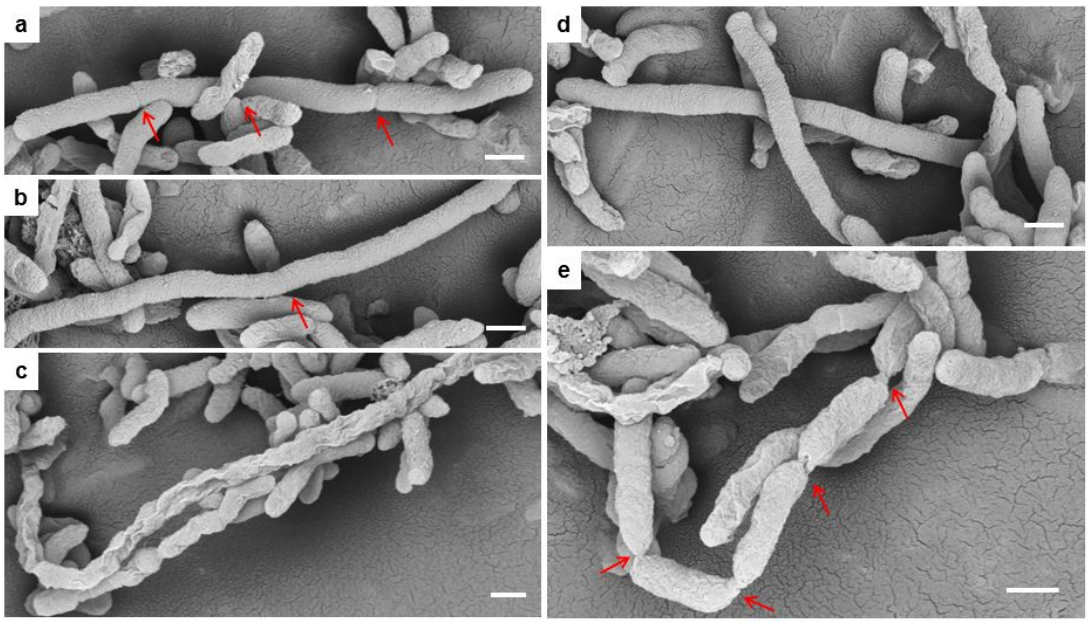

706 **Figure 3.** SEM images for *Xoo* after incubated in 25 μg/mL of compound $\mathbf{G_8}$, scale

707 bars for (a-e) are 500 nm.

708

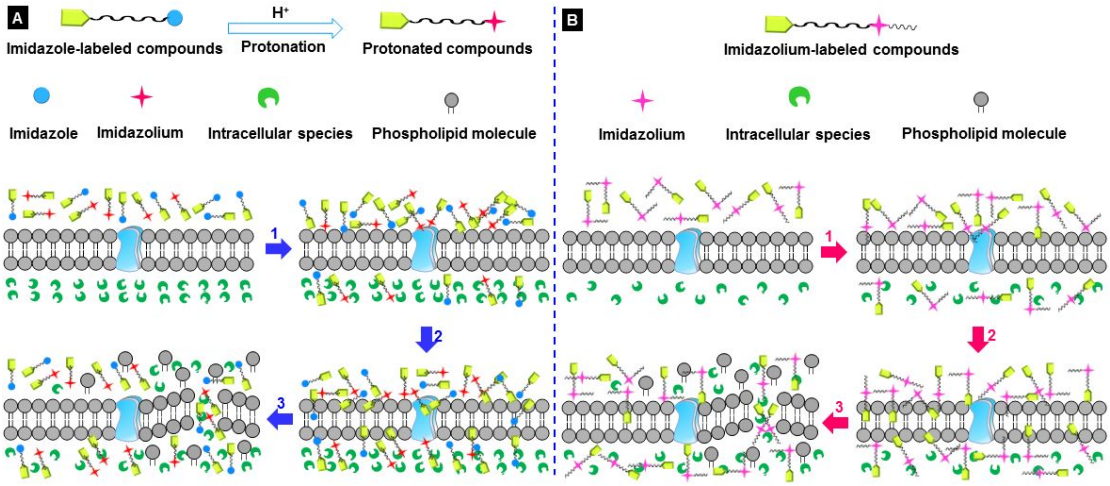

709 **Figure 4.** A proposed action mechanism for 1,3,4-oxadiazole thioethers bearing

710 imidazole groups (A) or imidazolium scaffolds (B) against plant pathogens.

712 **Graphical Abstract**

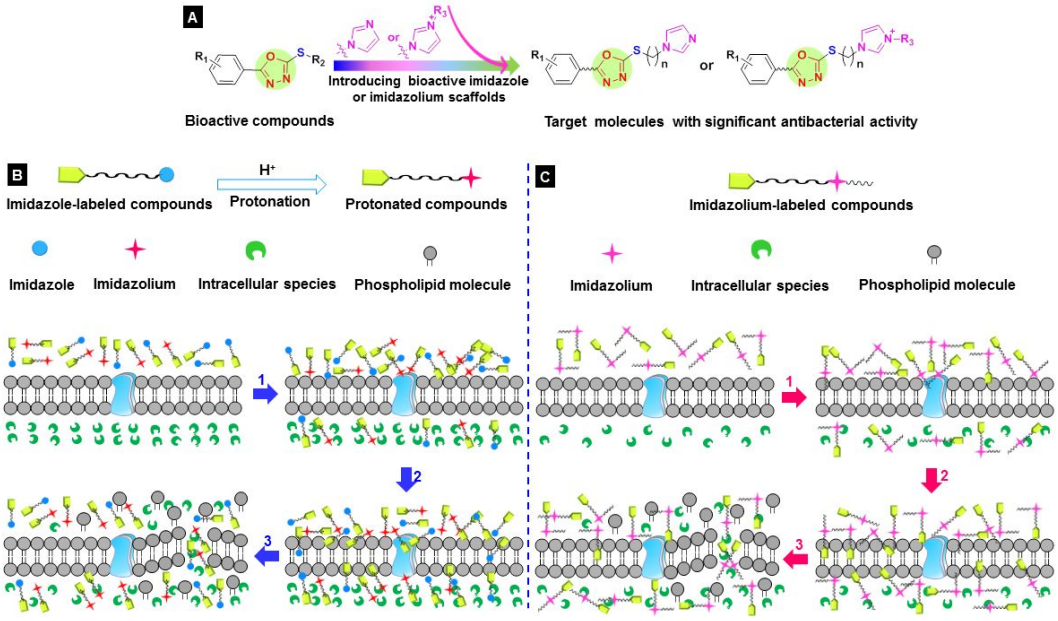

713

714 A series of imidazole (or imidazolium)-labeled 1,3,4-oxadiazole thioethers were
715 fabricated. Bioassay results indicated that the most antibacterial efficacy was
716 dramatically increased by approximately 314- and 127-fold against destructive plant
717 pathogens *Xoo* and *Xac* in comparison with those of mainly used commercial agents
718 **BT** and **TC**, respectively. This finding suggested that this kind of compounds can be
719 further explored and developed as promising indicators for the development of
720 commercial drugs. Moreover, a plausible action mechanism for attacking pathogens
721 was proposed based on the concentration dependence of SEM, TEM, and FM images.
722 Given the highly efficient bioactivity, imidazole (or imidazolium)-labeled
723 1,3,4-oxadiazole thioethers can be further explored and developed as promising
724 indicators for the development of commercial drugs.